

Directing Precursor Flux to Optimize *cis,cis*-Muconic Acid Production in *Saccharomyces cerevisiae*.

Shoham Mookerjee

A Thesis
in
The Department
of
Biology

Presented in Partial Fulfillment of the Requirements
for the Degree of Master of Science (Biology) at
Concordia University
Montreal, Quebec, Canada
December 2015

© Shoham Mookerjee, 2015

CONCORDIA UNIVERSITY

School of Graduate Studies

This is to certify that the thesis prepared

By: Shoham Mookerjee

Entitled: Directing Precursor Flux to Optimize *cis,cis*-Muconic Acid
Production in *Saccharomyces cerevisiae*.

and submitted in partial fulfillment of the requirements for the degree of
Master of Science (Biology)

complies with the regulations of the University and meets the accepted standards with
respect to originality and quality.

Signed by the final Examining Committee:

_____ Chair

Chair's name

_____ Examiner

Dr. Joanne Turnbull

_____ Examiner

Dr. Malcolm Whiteway

_____ Examiner

Dr. Justin Powlowski

_____ Supervisor

Dr. Vincent Martin

Approved by _____

Chair of Department or Graduate Program Director

_____ 2015

Dean of Faculty

ABSTRACT

cis, cis Muconic acid (CCM) is a compound that can be chemically converted to adipic acid, a major component of several copolymer plastics. Biological CCM-producing pathways with high yields have been characterized in *Escherichia coli*; however the downstream extraction process is prohibitively expensive at an industrial scale. *Saccharomyces cerevisiae* is a better industrial production host for organic acids; however biological CCM-producing pathways in *S. cerevisiae* have been plagued with significantly lower yields as compared to production in *E. coli*. In this thesis CCM production was explored in *S. cerevisiae* by construction of a heterologous pathway expressing AroZ from *K. pneumoniae*, AroY from *P. anserina* and Hqd2 from *C. albicans*, which resulted in the production of 2.9 mg/L of CCM. Accumulation of a native metabolite, shikimate, was observed, implying inefficient channeling of carbon into the heterologous pathway. To test this hypothesis, the diversion of carbon flux into the heterologous pathway was explored by modulation of the pentafunctional Aro1 protein. Replacing the wild-type *aro1* gene with a mutant version eliminated the accumulation of shikimate and increased the carbon flux into the heterologous pathway by 59%. In addition, two-step fermentations with aerobic and anaerobic phases were explored demonstrating the imbalance in oxygen requirements in the heterologous CCM pathway and ways to overcome it.

ACKNOWLEDGEMENTS

I would like to firstly thank my supervisor Dr. Vincent Martin for giving me the opportunity to work and learn in his lab. It has been an invaluable learning experience and I would not have been able to do it without his mentorship and guidance on academic and entrepreneurial life.

I would like to thank my committee members Dr. Malcom Whiteway and Dr. Joanne Turnbull for reading my thesis and helping me along the way.

I would also like to thank Nicholas Gold for helping me learn about HPLC and MS quantification; Dr. Kane LaRue, Damien Biot-Pellier and Lauren Narcross for their experimental set-up help; Elena Fossati for her extremely helpful presence around the lab; and Audrey Morin for keeping us fully stocked with reagents and all the official letters one needs. I would especially like to thank Mindy Melgar for her help in cloning the most important plasmid in this study!

I am also extremely grateful to my parents, Abhijit and Sudatta Mookerjee, whose unending patience and support have allowed me to get this far in life.

Lastly and definitely not leastly, I would like to thank the entire Martin lab and Walsh lab members for their support and friendship without which I would have never made it.

Also shout out to Whiskey and Caramel.

Contents

LIST OF FIGURES:.....	vii
LIST OF TABLES.....	viii
LIST OF ABBREVIATIONS:	ix
1. INTRODUCTION.....	1
1.1 Plastics and Chemical Synthesis.....	1
1.2 Biological Production of Muconic Acid.....	3
1.2.1 Natural Microbial Production of Adipic and Muconic Acids.....	4
1.2.2 The Chorismate Pathway.....	5
1.2.3 Heterologous Production of Muconic Acid in <i>Escherichia coli</i>	7
1.2.4 Heterologous Production of Muconic Acid in <i>Saccharomyces cerevisiae</i>	10
1.3 Molecular Channeling and Co-localization.....	13
1.3.1 Why is Metabolite Channeling and Enzyme Co-localization Important?.....	13
1.3.2 Metabolite Channeling and Co-localization in Aro1 Homologs.....	14
1.4 Rationale and Proposed Metabolic Engineering Objectives.....	20
1.4.1 Deletion of Aro1 to Increase Accumulation of 3-Dehydroshikimate.....	20
1.4.2 Mutating <i>aro1</i> to Remove Shikimate Dehydrogenase Functionality to Accumulate 3-Dehydroshikimate.....	21
1.4.3 Reducing the Abundance of Aro1 to Increase 3-dehydroshikimate Accumulation.....	21
2. MATERIALS AND METHODS.....	23
2.1 Strain and Plasmid Construction.....	23
2.1.1 Construction of Plasmid Expressing Recombinant CCM Pathway.....	23
2.1.2 Yeast Genes Deletion.....	28
2.1.3 Modification of Chromosomally Encoded Aro1.....	29
2.2 Strain Growth and Fermentation Conditions.....	31
2.3 Metabolite Identification and Analysis.....	32
3. RESULTS.....	32
3.1 Removing Feed-back Inhibition in the Chorismate Pathway.....	32
3.2 Deletion of Aro1 and its Effect on DHS Accumulation.....	33
3.3 Effect of Mutations in Aro1 on Cellular DHS Accumulation.....	39

3.4 Effect of Decreasing the Abundance of Aro1 on DHS Accumulation.....	40
3.5 Effect of Optimizing DHS Accumulation on Carbon Flux into Heterologous CCM Pathway	45
3.5.1 Effect of Complete De-Regulation of the Chorismate Pathway on CCM Production ..	47
3.5.2 Effect of Ablation of Aro1 Functionality on Carbon Flux Towards CCM Production ...	47
3.5.3 Effect of Aro1 ^{K1370L} Mutation on Carbon Flux Towards CCM Production	48
3.5.4 Effect of Decreasing Aro1 Abundance on Carbon Flux Towards CCM Production	49
3.6 Accumulation of Fermentation By-Products as Unwanted Carbon Sinks.....	51
3.7 Exploring the Effect of Two-step Fermentation of K341 on CCM and PCA Production	54
3.8 Effect of Oxygenation on PCA, Catechol and CCM Production.....	57
4. DISCUSSION.....	60
5. CONCLUSION.....	67

LIST OF FIGURES:

Figure 1.	Chemical synthesis of adipic acid.....	2
Figure 2.	Diagram of chorismate pathway and heterologous production of <i>cis, cis</i> muconic acid and associated native <i>S.cerevisiae</i> metabolism.....	6
Figure 3.	Comparison of <i>A. thaliana</i> DHQ-SDH protein and homologous domains of <i>S. cerevisiae</i> Aro1.....	16
Figure 4.	Representation of internal structure of Aro1 homo-dimer.....	17
Figure 5.	Representation of experimental plan for this study.....	19
Figure 6.	Model of the <i>Haemophilus influenzae</i> AroE shikimate dehydrogenase active site.....	22
Figure 7.	<i>In vivo</i> mutagenesis of shikimate dehydrogenase domain of Aro1.....	30
Figure 8.	Comparison of growth and metabolite accumulation by strains K34 pEV, K34 p4BD, 13D pEV and 13D p4BD.....	35
Figure 9.	Effects of varying concentrations of dropout media supplementation and evolutionary adaptation on growth profiles of K341.....	37
Figure 10.	Comparison of growth and metabolite accumulation by strains K341 pEV, K341 p4BD, 13D pEV and 13D p4BD.....	38
Figure 11.	Comparison of growth and metabolite accumulation by strains K34M pEV, K34M p4BD, 13D pEV and 13D p4BD.....	41
Figure 12.	Comparison of growth and metabolite accumulation by strains K34Cln2 pEV, K34Cln2 p4BD, 13D pEV and 13D p4BD.....	43
Figure 13.	Comparison of the maximum accumulation of shikimate and 3-dehydroshikimate (DHS) in 13D p4BD, K34 p4BD, K341 p4BD, K34M p4BD and K34Cln2 p4BD.....	44
Figure 14.	Comparison of growth and metabolite accumulation by strains 13D p6g, K34 p6g, K341 p6g, K34M p6g and K34A1Cln2 p6g.....	46
Figure 15.	Comparison of the maximum accumulation of shikimate and protocatechuic acid (PCA) in <i>cis, cis</i> -muconic acid-producing strains.....	50
Figure 16.	Comparison of ethanol and acetate production by strains 13D, K34, K341, K34M and K34A1Cln2.....	52
Figure 17.	Comparison of growth and metabolite accumulation by K341 p6g in a two-step fermentation process.....	56
Figure 18.	Comparison of growth and metabolite accumulation by 13D pDAC in an aerobic and anaerobic fermentation process.....	59

LIST OF TABLES

Table 1. Plasmids and strains used in this study and their corresponding genotypes.....	24
Table 2. Primers and other guide-RNA sequences used in this study.....	25
Table 3. Investigation of growth conditions of <i>Δaro1 S. cerevisiae</i> strains.....	34
Table 4. Titters and yields of metabolites in <i>cis,cis</i> -muconic acid-producing <i>S.cerevisiae</i> strains.....	64

LIST OF ABBREVIATIONS:

(In order of appearance)

CCM: *cis,cis*-muconic acid

E4P: Erythrose-4-phosphate

PEP: Phosphoenolpyruvate

DHS: 3-Dehydroshikimic acid

DAHP: 3-deoxy-D-arabino-heptulosonate 7-phosphate

DHQ: 3-dehydroquinic acid

S3P: Shikimate-3-phosphate

5-EPS: 5-enol-pyruvyl-shikimate-3-phosphate

DHSD: Dehydroshikimate dehydratase

PCA: Protocatechuic acid

PCAD: Protocatechuic acid decarboxylase

CDO: Catechol-dioxygenase

ADO: Anthranilate 1,2 dioxygenase

SMO: salicylate 1-monoxygenase

SA: Salicylic acid

ICS: Isochromate synthase

IPL: Isochromate pyruvate lyase

2,3 DHB: 2,3 –dihydrobenzoic acid

NADP+: Nicotinamide adenine dinucleotide phosphate

NADPH: Reduced form of nicotinamide adenine dinucleotide phosphate

PEST: Proline, Glutamine, Serine, Threonine

GFP: Green Fluorescent Protein

PCR: Polymerase Chain Reaction

CRISPR: Clustered Regularly Interspaced Short Palindromic Repeats

1. INTRODUCTION

1.1 Plastics and Chemical Synthesis

Plastic is ubiquitously used in most facets of life such as cars, packaging, clothing and food to name a few. There are many different types of plastic such as polyvinylchloride, polystyrene, and nylon each with their own specific uses. The commonality in plastics is that they are mostly synthetic polymers of combinations of different monomeric building blocks. The variations in the chemistry of the building blocks lead to the different properties of plastic. These building blocks range from chlorinated compounds such as vinyl chloride, aromatics molecules such as styrene, amines and dicarboxylic acids. This study focuses on the di-carboxylic acids monomers, specifically *cis,cis*-muconic acid (CCM).

cis,cis-Muconic acid is an unsaturated six carbon di-carboxylic acid¹. It can be chemically hydrogenated to produce saturated adipic acid which is one of the most industrially relevant chemical building blocks today². Adipic acid is on the list of the 50 top bulk chemicals produced with a worldwide production of nearly 3 million tonnes². It is used in the production of nylons, lubricants, coatings for the chemical, pharmaceutical and food industries^{3,4}. Adipic acid is presently manufactured from benzene, a carcinogenic derivative of the Benzene, Toluene and Xylene (BTX) fraction of petroleum⁵. Benzene is reduced at high temperatures and pressures to cyclohexane. Cyclohexane undergoes two oxidation steps under high pressure and temperature to yield a mixture of cyclohexanol and cyclohexanone. This mixture is further reacted in air and excess nitric acid and a copper or vanadium catalyst to produce adipic acid (Figure 1). This process is dependent on benzene and other petroleum derived feedstocks which are not limitless and have supply stability problems⁶. In the last five years the costs of a barrel of crude oil has varied from \$120 to \$50⁷; this drastic price fluctuations can have significant impact of the production costs of plastics⁸. As the stability of oil production is further damaged by continuous conflict in oil producing countries, and by the inevitable depletion of the finite petroleum supply, the costs of producing plastics will be detrimentally affected. The chemical

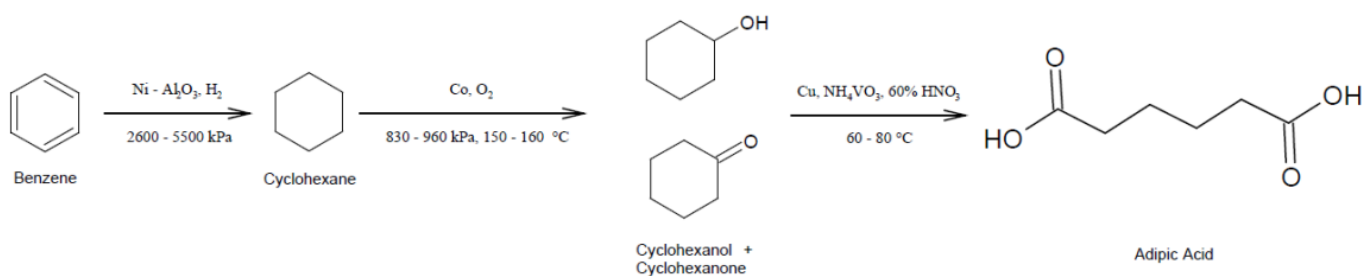


Figure 1. Chemical synthesis of adipic acid. Benzene is reduced at pressure in the presence of a nickel catalyst to form cyclohexane. Cyclohexane is oxidized in the presence of a cobalt catalyst and high pressure and temperature to form a mixture of cyclohexanol and cyclohexanone. This mixture is further reacted with nitric acid and a copper catalyst at high temperature to form adipic acid ⁵.

synthesis of adipic acid is also extremely energy intensive as the reactions need to be maintained under high pressure and temperature⁹. The nitric acid involved in the reduction of cyclohexanol and cyclohexanone to adipic acid is also extremely unsustainable. Nitric acid is made from ammonia, under high pressure and temperature making it an energy and cost intensive manufacturing process. It is estimated that around 10% of the world's total nitric acid production is used in the synthesis of adipic acid¹⁰. As about 2% of the world's energy production is used for the production of ammonia using the Haber process, it can be deduced that the production of adipic acid accounts for about 0.2% of the world's entire energy production every year.

Chemical production of adipic acid has negative environmental consequences as well. There is a large amount of NO_x (NO₂, N₂O) emissions in the nitric acid assisted ring-opening step; life cycle analyses have shown that production of adipic acid is responsible for the production of nearly 10% of the world's anthropogenic production of NO_x gas^{11,12}. NO_x is a potent greenhouse gas and has a severe effect on global warming¹¹. Production of adipic acid also uses benzene, a known carcinogen¹³ and produces NO₂ which has been implicated in respiratory illnesses¹⁴. Thus, the chemical synthesis of adipic acid is not economically, energetically or environmentally sustainable by any metric.

1.2 Biological Production of Muconic Acid

In the past two decades, biological methods for producing fuels and chemicals have become mainstream and commercially feasible¹⁵. Metabolic engineering is the ability to modify and add to the genomes of microorganisms to allow them to produce novel, heterologous and industrially or medically relevant chemicals^{16,17}. Biological engineering has been used to produce fuels^{18,19}, plastics such as polyhydroxyalkanoates (PHA), poly-3-hydroxybutyrates (PHBs) and polyethylene^{20,21}, food additives^{22,23}, pharmaceuticals²⁴ and medicinal compounds^{25,26} and is taking over as alternative to large scale chemical production. As the feedstocks for microbial fermentation are renewably produced²⁷⁻²⁹ there are few supply problems. Also, as the growth and fermentation usually occurs at a temperature range of 30-37

°C the process is not very energy intensive and there are very few toxic by-products. To continue to produce industrial scales of adipic acid, a biological production option is the most desirable way forward.

1.2.1 Natural Microbial Production of Adipic and Muconic Acids

The production of adipic acid via the biological degradation of cyclohexane and cyclohexanol has been reported in multiple bacterial strains such as *Acinetobacter* sp³⁰ and *Pseudomonas* sp³¹. The degradation pathways of cyclohexanol and cyclohexanone include multiple characterized genes such as cyclohexanol dehydrogenases³² and monooxygenases³³ and have been under investigation for quite some time. Addition of these heterologous gene clusters to *E. coli* supplemented with cyclohexanol and cyclohexanone have resulted in trace amounts of adipic acid produced³⁰. However, given the fact that cyclohexanol is a petroleum-derived feedstock and the yield of adipic acid from its biological degradation is low it is not a feasible pursuit.

Benzoate has also been used as a feedstock to produce biological adipic acid. This uses the bacterial β -ketoadipate pathway found in most species of soil bacteria such as *Pseudomonas*³⁴, *Burkholderia*³⁵ and *Acinetobacter*³⁶. This pathway catalyzes the catabolism of benzoate into succinyl-coA and acetyl-coA via intermediates catechol and protocatechuic acid. Catechol is the branch-point in this pathway and can be subsequently cleaved by catechol-1,2-dioxygenase³⁷ into *cis,cis*-muconic acid (CCM). CCM can be chemically hydrogenated with a platinum catalyst to produce adipic acid³⁸. *Pseudomonas* strains that have been grown under fed-batch conditions with supplemented benzoate produced CCM at a yield of 91%³⁹. This process was further optimized by controlling oxygen supply resulting in high cell density fermentation that produced 44 g/L of CCM⁴⁰. However, as benzene is toxic and inhibitory to cell growth at high concentrations and is a petroleum-derived feedstock, it is not the ideal production method to replace chemical synthesis of adipic acid. A direct conversion of glucose or similar renewable, non-toxic feedstock to adipic acid would be ideal.

1.2.2 The Chorismate Pathway

Biological production of adipic acid using glucose as a starting substrate would require a native pathway that was capable of producing similar molecules. As benzene and cyclohexane are aromatic molecules, a cell's native aromatic molecule producing pathway would be ideal to make precursors for the production of CCM. The most common aromatic producing pathway in microorganisms, both prokaryotic and eukaryotic, is the chorismate pathway⁴¹.

The chorismate pathway is ubiquitous in most clades of life, however, its organization and structure is variable⁴². The basic chorismate pathway converts erythrose-4-phosphate (E4P) and phosphoenolpyruvate (PEP) into aromatic amino acids and molecules such as tyrosine and *p*-aminobenzoic acid via several well characterized steps. The bacterial chorismate pathway is composed of multiple mono-functional enzymes that catalyze the conversion of E4P and PEP to chorismate with 3-dehydroshikimate (DHS) as an intermediate (Figure 2). All subsequent naming of the catalytic activities of the enzymes in this pathway will follow the bacterial system for convenience unless otherwise stated. The DAHP synthase activity catalyzed by AroF or AroG condenses E4P and PEP to produce 3-deoxy-D-arabino-heptulosonate 7-phosphate (DAHP). DAHP is cyclized to form 3-dehydroquinase (DHQ) by a 3-dehydroquinase synthase activity catalyzed by AroB. DHQ is subsequently converted to 3-dehydroshikimic acid (DHS) by a 3-dehydroquinase encoded by AroD. DHS is reduced to form shikimic acid via the shikimate dehydrogenase AroE. Shikimate kinases, AroK and AroL, add a phosphate group to shikimic acid to produce shikimate-3-phosphate (S3P). S3P is converted into 5-enol-pyruvyl-shikimate-3-phosphate (5-EPS) by 5-EPS synthase activity that is encoded by AroA⁴³. 5-EPS is finally converted to chorismate by a chorismate synthase, AroC. Chorismate is then further converted into amino acids and vitamins by a multitude of enzymes. This organizational structure, with mostly distinct enzymes for each functionality, is also seen in plants, where the chorismate pathway is mostly active in plastids, that have bacterial origins⁴⁴.

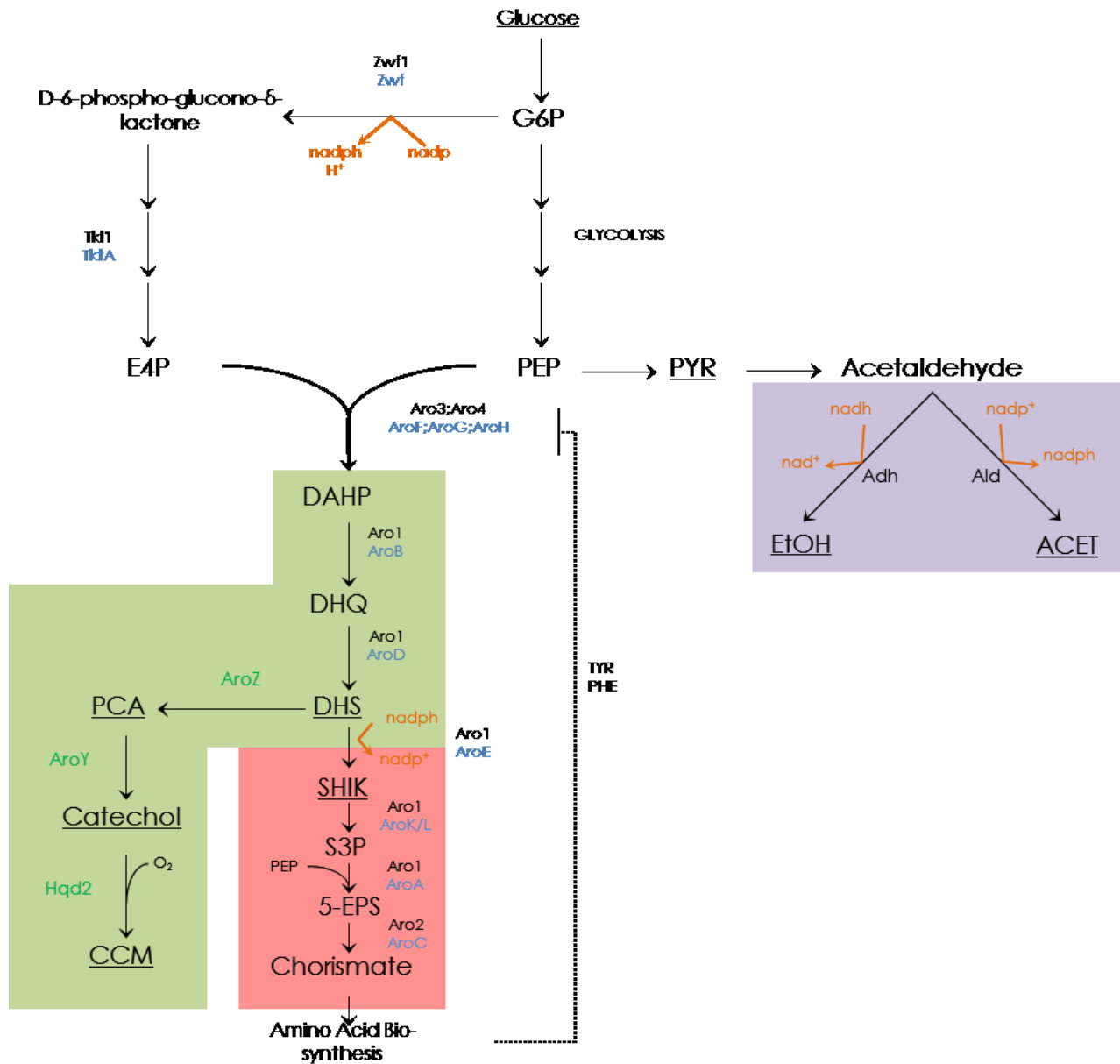


Figure 2. Diagram of chorismate pathway and heterologous production of *cis*, *cis*-muconic acid and associated native *S. cerevisiae* metabolism. The native *S. cerevisiae* genes are labeled in black and the homologous *E. coli* genes are in blue. The heterologous genes indicating the 3-dehydroshikimate dehydrogenase (*aroZ*) from *K. pneumoniae*, the protocatechuic acid decarboxylase (*aroY*) also from *K. pneumoniae* and the catechol-dioxygenase (*hqd2*) from *C. albicans* are marked in green. The redox cofactors are marked in orange. The dashed lines represent allosteric feedback inhibition of Aro4 and Aro4 by tyrosine and phenylalanine, respectively. The underlined metabolites have been measured in this study. The green shading outlines the desired flow of carbon into the heterologous CCM pathway. The red shading outlines the native consumption of the pre-cursor DHS for aromatic molecule synthesis. The purple shading outlines metabolites previously known to accumulate during fermentation (carbon sinks).

Compared to prokaryotes, where all the steps in the chorismate pathway are catalyzed by mono-functional enzymes, the steps from AroB to AroA are catalyzed by one pentafunctional polypeptide in eukaryotes⁴². In *S. cerevisiae*, this is the Aro1 polypeptide. Through phylogenetic analysis, it was observed that this is an ancient eukaryotic invention and is widespread in all lower eukaryotes and protozoans⁴². It has been proposed that the pentafunctional polypeptide probably arose through multiple gene fusions as its catalytic domains can be mapped by homology to the singular prokaryotic proteins⁴⁵. Interestingly, the chorismate pathway is completely absent from metazoans including humans; these organisms rely on acquiring aromatic molecules through their diet.⁴²

The chorismate pathway is the gateway to produce all the aromatic molecules present in a cell ranging from amino acids, such as tyrosine, tryptophan and phenylalanine, to vitamins such as folates, and has also been demonstrated to produce heterologous secondary metabolites such as vanillin⁴⁶ and styrene⁴⁷. Thus, the chorismate pathway is central to cellular metabolism and is capable of shuttling large amounts of carbon. Modifying this pathway to produce industrial scales of CCM or adipic acid would appear to be a sensible choice.

1.2.3 Heterologous Production of Muconic Acid in *Escherichia coli*

The first semi-biological pathway to produce adipic acid from glucose (Figure 2) was engineered in *Escherichia coli* by K.M. Draths and J.W. Frost in 1994⁴⁸. The production of adipic acid was a two-step process in which *cis,cis*-muconic acid was produced at titers of 2.37 g/L via *E. coli* fermentation and extracted; subsequently the CCM was chemically reduced to produce adipic acid at a 90% efficiency. This *E. coli* strain did not natively produce CCM and was rationally engineered and complemented with heterologous enzymes. The native chorismate pathway used for aromatic amino acid biosynthesis was modulated to accumulate the precursor DHS which was then converted to CCM via three heterologous proteins. Upon optimization of central carbon-metabolism and the chorismate pathway, CCM titers of 36.8 g/L were achieved⁹.

The optimization of CCM production was achieved through multiple pathway modifications. The chorismate pathway is ubiquitous in bacteria, fungi and plants and has been extensively

studied^{43,49,50}. This pathway uses PEP and E4P from glycolysis and the pentose phosphate pathway and condenses them to form DAHP. This marks the first committed step in the chorismate pathway and is catalyzed by 3 isozymes, the major one being AroF in prokaryotes^{43,48}. AroF and its isozymes are feedback inhibited by tyrosine and phenylalanine limiting the carbon flux into the pathway. Niu *et al.* overcame this inhibition by over-expressing a copy of feedback inhibition resistant AroF^{fbr}^{51,52} on a plasmid and disrupting the native *aroF* promoter^{53,52}. Increasing the flux through the chorismate pathway by eliminating feedback inhibition resulted in the accumulation of DAHP which was alleviated by expressing a second copy of the native *aroB* gene encoding a 3-dehydroquinate synthase⁵². To accumulate 3-dehydroshikimate the *aroE* gene encoding shikimate dehydrogenase, which converts DHS to shikimate, was deleted. The resulting strain, although accumulating large amounts of DHS, was unable to produce aromatic molecules and its growth media needed to be supplemented with the aromatic amino acids and vitamins⁵². The accumulated DHS was converted to protocatechuic acid by expression of 2 copies of heterologous *aroZ* gene from *Klebsiella pneumoniae* encoding a DHS dehydratase (DHSD). Protocatechuic acid (PCA) was subsequently decarboxylated to catechol by a heterologous PCA decarboxylase (PCAD) *aroY*, also from *K. pneumoniae*. Catechol finally underwent a ring-opening catalyzed by catechol-1,2-dioxygenase (CDO) expressed by the *catA* gene from *Acinetobacter calcoaceticus* resulting in 17 g/L of CCM. To improve yields the pentose phosphate pathway was up-regulated by expressing multiple copies of the native transketolase TktA⁵⁰. Additionally, an extra copy of *catA* was maintained on a plasmid creating a CCM overproducing strain. This strain was grown under high oxygen fermentation to finally yield 36.8 g/L of CCM. The clarified broth containing CCM was hydrogenated under high pressure hydrogen gas and a platinum catalyst to produce adipic acid at 97% efficiency³⁸.

Recently, three other routes to CCM have been discerned and demonstrated in *E. coli*, all derived from the chorismate pathway. In 2013, Sun *et al.* demonstrated a novel biosynthesis pathway for CCM production via the tryptophan precursor anthranilate⁵⁴. Anthranilate is derived from the chorismate pathway and is the first intermediate in tryptophan biosynthesis⁴¹. Anthranilate-1,2-dioxygenase (ADO) catalyzes the conversion of anthranilate to

catechol which is subsequently converted into *cis,cis*-muconic acid via a catechol-1,2-dioxygenase (CDO). Multiple ADO's and CDO's were screened *in vivo* and the ADO, PaantABC, from *Podospora aeruginosa* and the CDO, CatA, from *Podospora putida* were chosen. Upon up-regulation of carbon flux through the chorismate pathway by alleviating feedback-inhibition, as previously mentioned⁹, 389.96 mg/L of CCM was produced in a 32-hr fermentation in shake-flasks.

A year later, in 2014, the same group reported another novel CCM biosynthetic route⁵⁵. In this route, chorismate was shunted to isochorismate via an isochorismate synthase (ICS)⁵⁶. Isochromate was then converted to salicylic acid (SA) via an isochromate pyruvate lyase (IPL)⁵⁷. A salicylate-1-monoxygenase (SMO) catalyzed the conversion of salicylic acid to catechol, which was finally converted to CCM via a CDO. In order to increase the availability of chorismate, *pheA* and *tyrA*, genes encoding proteins that funnel chorismate into phenylalanine and tyrosine biosynthesis, were deleted. Coupled with overexpression of TktA, PpsA, AroG^{fbr}⁵⁸ (an isozyme of AroF), EntC⁵⁸ (an ICS from *E. coli*) and PchB⁵⁸ (an IPL from *Pseudomonas fluorescens*) 1.2 g/L of SA was produced. Out of the multiple SMO's screened *in vivo*, codon-optimized NagH from *P. putida* was chosen as the best candidate to convert SA to catechol. Catechol was finally converted to CCM upon the addition of the *catA* gene⁵⁴ from *P. putida*. After flux balancing through plasmid copy number optimization a strain producing 1.4 g/L of CCM was created.

The isochorismate shunt from the chorismate pathway was also recently used by Wang *et al.* in 2015 to create another novel CCM producing *E. coli* strain⁵⁹. In this strain, isochorismate was converted to 2,3 dihydrobenzoic acid (2,3-DHB) by EntBA⁶⁰ from *K. pneumoniae*. 2,3-DHB was converted to catechol by a 2,3-DHB decarboxylase, EntXp, also from *K. pneumoniae*⁶⁰. Upon addition of CatA from *P. putida* and over-expression of the chorismate pathway 608 mg/L of CCM was produced.

1.2.4 Heterologous Production of Muconic Acid in *Saccharomyces cerevisiae*

Even though these engineered *E. coli* strains produce large amounts of CCM, the process is very expensive for industrial scale-up. As *E. coli* grow and ferment under strictly neutral pH's any organic acids that are produced are produced as salts. Extraction of the un-dissociated acids from the salts requires high levels of acidification of the broth and subsequent precipitation and desalting steps. A large amount of salt and calcium carbonate waste is produced in this step and is quite prohibitive at industrial scales. Additionally, *E. coli* fermentations and cultures are susceptible to phage contamination, which destroys the fermentation process and is extremely difficult to eradicate for subsequent fermentations. This adds a lot of cost and risk in the production process. In response to this, there is a recent trend in biological production to use a more robust organism such as *Saccharomyces cerevisiae* for industrial scale production.

S. cerevisiae or Baker's yeast is one of the best studied model organisms⁶¹. It is highly tractable with a large repertoire of genetic tools to add to, remove and modulate the functionality of the cells¹⁷. It is also generally regarded as safe and is highly resistant to viral infections⁶². Yeasts are also tolerant to multiple forms of chemical and fermentative inhibitors and have been demonstrated as robust and efficient microbial production hosts⁶³⁻⁶⁶.

Weber *et al.* in 2012 demonstrated the proof of concept of the heterologous pathway developed by Niu *et al.* in *S. cerevisiae*⁶⁷. Multiple homologs, both codon-optimized and un-optimized, for each of the heterologous steps were screened via *in vivo* testing. Through this analysis, the DHSD expressed by codon-optimized *aroZ* gene from *Podospora anserina* (also known as *P. pauciseta*), the PCAD encoded by the codon-optimized *aroY* gene from *K. pneumonia* and the CDO expressed by *catA* from *Acinetobacter radioresistens* were chosen. In order to accumulate DHS, the native chorismate pathway was modified in a way similar to what Niu *et al.* did in *E. coli* with the deletion of *aroE*. In *E. coli* and most other prokaryotes the seven chorismate pathway reactions are catalyzed by seven distinct enzymes and the deletion of any of the enzymes leads to the accumulation of its substrate⁴³. Thus, the deletion of *aroE*, which catalyzes the reduction of DHS to shikimic acid, leads to the accumulation of DHS. In

eukaryotes, specifically *S. cerevisiae*, the seven enzymatic steps of the chorismate pathway are catalyzed by only three enzymes⁴¹. Aro4 and its paralog Aro3 condense E4P and PEP to produce DAHP. The next five steps from DAHP to 5-enolpyruvyl shikimate-3-phosphate (5-ESP) are catalyzed by a single protein Aro1. Aro2 catalyzes the conversion of 5-ESP to chorismate. The Aro1 protein is a pentafunctional protein with 5 different active sites all fused into one protein⁶⁸. The five distinct chorismate forming enzymes in *E. coli* can be aligned using homology to the Aro1 protein. The shikimate dehydrogenase domain responsible for catalyzing the conversion of DHS to shikimic acid is located at the 3' or N-terminal of Aro1⁶⁸. Weber *et al.* replaced the entire domain with a stop codon, effectively removing shikimate dehydrogenase activity from Aro1⁶⁷. With this modification and the expression of the screened heterologous enzymes 1.56 mg/L of CCM was produced. This titer is considerably lower than the 36.8 g/L of CCM as reported by Niu *et al.* in *E. coli*. However, Weber *et al.* did not alleviate the feedback inhibition in the chorismate pathway and there was no attempt at flux balancing to improve metabolite conversion in the strains.

The optimization of this pathway in *S. cerevisiae* was performed by Curran *et al.* in 2013⁶⁹. Multiple codon-optimized and non-codon optimized enzymes for all three of the heterologous activities were tested *in vivo*. Finally, a DHSD, *aroZ*, from *P. anserina*; a PCAD, *ecI_01944*, from *Enterobacter cloacae* and a CDO, *hqd2*, from *Candida albicans* were selected to construct the CCM pathway. Curran *et al.* alleviated the feedback inhibition in the chorismate pathway by deregulating the endogenous DAHP synthase activity by deleting the *aro3* and *aro4* genes and over-expressing a chromosome-integrated copy of the feedback inhibition resistant mutant Aro4^{K229L} as previously described by Luttick *et al.*⁴⁹. Expressing the heterologous enzymes in this aromatic pathway deregulated strain achieved a CCM titer of 21 mg/L. However, it was observed that there was a significant bottleneck in the heterologous pathway as there was an accumulation of 166 mg/L of PCA in this strain. This was addressed by expressing the PCAD on a high copy plasmid and integrating multiple copies of the PCAD using Ty2 retro-transposon δ elements found throughout the genome. The over-expression of the PCAD in conjunction with the over-expression of the other heterologous genes in a feedback inhibition resistant strain resulted in a CCM titer of 30 mg/L. Subsequently, metabolic flux-balance analysis was used to

further optimize yields of CCM. *In silico* flux balance analysis has been widely used to identify (and eliminate) competing reactions and channel more carbon flux through the desired pathway⁷⁰⁻⁷⁴. An extant yeast genome model, iMM904⁷⁵, was used and modified to include the three heterologous reactions. The model predicted a 60.9% mol/mol glucose yield of CCM on channeling carbon into the pentose phosphate pathway through the transketolase activity^{9,76} instead of the oxidative branch of the pentose phosphate pathway which would result in the balance of availability of precursors E4P and PEP. It would also remove a major source of NADPH in the cell, which is required for the conversion of DHS to shikimate. In order to achieve this, Curran *et al.* deleted the glucose-6-phosphate dehydrogenase, *zwf1*, and over-expressed the native transketolase, *Tlk1*, on a high copy plasmid in the feedback inhibition resistant strain to create strain MU11. However, as the bottleneck of accumulating PCA was still present, multiple genomic integrations of PCAD were made in strain MU11 to create strain MU12 with a dramatically increased PCAD RNA transcript. Further over-expression of the DHSD, PCAD and CDO on high copy plasmids in strain MU12 resulted in a CCM titer of 77 mg/L with a yield of 3.9 mg/g glucose. Finally, MU12 was grown on modified synthetic complete media with 40 g/L glucose for an extended period of 108 hrs. The final CCM titer in this strain was 141 mg/L, which represents an impressive 90-fold optimization over the strain reported by Weber *et al.*

Recently, Horwitz *et al.* demonstrated the production of 2.7 g/L of PCA in a modified *S.cerevisiae* strain⁷⁷. This was done by deletion of the entire *aro1* gene and replacing it with *aroF*, *aroB*, and *aroD* from *E. coli* to prevent the siphoning of DHS from the heterologous pathway. One copy of *aroZ* and five copies of *aroY* from *K. pneumoniae* and one copy of *catA* from *C. albicans* were integrated into the genome. As the deletion of *aro1* resulted in the strain unable to produce any aromatic amino acids, 2-step fermentation was carried out to produce CCM. The cells were grown in YPD for 48hrs to accumulate biomass and subsequently washed and added to minimal media containing 40 g/L of the disaccharide sucrose. This two-step fermentation created a simple switch mechanism between a biomass-accumulation step in rich media and a production phase in minimal media. However, no catechol and CCM were observed in this strain pointing to an uncharacterized defect in the sequence-verified,

integrated copies of the PCAD. Feeding the cells with 1 g/L of catechol resulted in the formation of unreported quantities of muconic acid.

Thus, it can be ascertained that *S. cerevisiae* has the potential to become a microbial host for the industrial production of adipic acid via *cis,cis*-muconic acid. The best-characterized biosynthetic route to CCM stems from the native chorismate pathway and is dependent on the precursor DHS. Although strides have been made to up-regulate the carbon flux going through the pathway^{43,46,49} there is still a roadblock to accumulation and availability of DHS. Weber *et al.* deleted the N-terminal domain of the pentafunctional Aro1 protein in an effort to disrupt the shikimate dehydrogenase catalytic function⁶⁷. However, this did not make any discernible effect on the amount of PCA produced. However, when this truncated version of Aro1 was over-expressed on a plasmid the titer of PCA increased 7-fold. A similar result was also achieved by over-expressing *E. coli* AroB and AroD in *E. coli* pointing to the AroB and AroD functionalities to be limiting. Curran *et al.* did not modulate the flux through the Aro1. However, deletion of endogenous *aro3* and *aro4* genes and over-expressing Aro4^{fbr} also accumulated 166 mg/L PCA. Thus alleviation of feedback inhibition and overexpression of AroB and AroD had similar effects on the amount of DHS being produced. From these data, we can conclude that there are several bottlenecks in the chorismate pathway and flux through the Aro1 protein is one of them. As described previously, given that most eukaryotes with the chorismate pathway have the pentafunctional Aro1 domain fusion it is possible there is an evolutionary reason for its persistence. Multiple enzymes could fuse together to increase the flux through the pathway by decreasing the need for diffusion of the substrates.

1.3 Molecular Channeling and Co-localization

1.3.1 Why is Metabolite Channeling and Enzyme Co-localization Important?

Intracellular environments differ markedly from the dilute solutions in which most *in vitro* experiments are conducted⁷⁸. Up to 30% of the cellular volume of *E. coli* is composed of macromolecules leading to a dense soup of lipids and proteins which dramatically slows down

diffusion and affects enzyme functionality⁷⁹. This molecular crowding leads to inefficient distribution and diffusion of substrates and free-floating enzymes, accumulation of toxic intermediates and loss of substrates to competing pathways. Many cellular pathways overcome this through substrate channeling by utilizing multi-enzyme complexes and protein co-localization^{80–82}.

Molecular channeling in natural systems is exemplified by tryptophan synthase, an $\alpha 2\beta 2$ complex⁸³. It channels the metabolic intermediate indole from the active site of the α subunit to the active site of the β subunit. The subunits arrange themselves to form a hydrophobic intramolecular tunnel that connects the adjacent active sites and has a diameter matching that of four molecules of indole. A number of ligand-induced conformational changes channels the indole and prevents it from diffusing into the cytosolic bulk or accumulating, which effectively increases the reaction rates by two orders of magnitude over the free, un-complexed subunits⁸⁴. Thus, a similar channeling mechanism could be the purpose of the pentafunctional Aro1 protein.

1.3.2 Metabolite Channeling and Co-localization in Aro1 Homologs

The metabolite-channeling hypothesis has been explored in the central chorismate pathway too. This hypothesis has been tested for the AroM enzyme in *Aspergillus nidulans*, which is a pentafunctional homolog of Aro1 from *S. cerevisiae*⁶⁸. Over-expression of a DHSD at 15-17 times its normal physiological levels led to an acute accumulation of PCA with a drastic reduction in the chorismate pathway intermediates⁸⁵. A flux control coefficient relates the n -fold change in PCAD enzyme concentration to the n -fold change in flux to PCA. The high accumulation of PCA demonstrates that AroM is extremely leaky and under normal condition *in vivo* the PCAD has a flux control coefficient of -1 for the chorismate pathway⁸⁶. This lack of substrate channeling can also be ascertained from the high accumulation of PCA seen in the *S. cerevisiae* strains developed by Curran *et al.* However, at much higher expression of the PCAD in *A. nidulans* it was shown that there is some basal metabolic channeling through AroM to preserve the production of aromatic molecules for cell viability⁸⁶.

Thus, if there is no direct metabolic channeling through Aro1 the evolutionary advantage could be based on increasing the local concentration of the substrates to increase the rate of substrate flux through the enzymatic complex. Enzyme co-localization is observed in many plant systems such as dhurrin and phenylpropanoid biosynthesis⁸⁰. In prokaryotes, as previously mentioned, the chorismate pathway is organized as mono-functional proteins that catalyze the individual reactions. However, in plants and fungi that is not the case. In plants the 3-dehydroquinase and shikimate dehydrogenase domains are organized as a single bi-functional protein domain fusion⁸⁷. The DHQ-SDH domain of *Arabidopsis thaliana* has been the most studied and demonstrates channeling in the pathway.

The DHQ and SDH proteins in the fusion protein are homologous to the bacterial enzymes so the system is highly conserved. Singh *et al.* crystallized the protein in the presence of shikimate, NADP⁺ and tartrate (a structural analogue of DHQ) and identified a monomeric functional state. The crystal structure of the protein revealed a concave architecture, which places the two enzyme active sites in close proximity of each other (Figure 3). This structure allows for an extremely processive SDH domain with a ~9-fold increase in turnover rates as compared to the DHQ domain or to a mono-functional SDH domain from prokaryotes. This validates the hypothesis of enzyme fusions promoting metabolite co-localization to increase carbon flux through the pathway.

AroM from the fungi *A. nidulans* has also been implicated in facilitating metabolite co-localization. Mutation studies of isolated and native 3-dehydroquinase domains demonstrate that the K_m/K_{cat} ratio of the DHQase in the pentafunctional complex is 50% higher than the ratio in singular isolated domains⁸⁸. Similarly, the catalytic effect of the isolated DHQase domain was 160-fold lower than the wild-type pentafunctional enzyme domain in *N. crassa*⁸⁹. Considering the AroM proteins from *A. nidulans* and *N. crassa* are homologs to *S. cerevisiae* we can safely conclude that there might be basal metabolite co-localization present in the chorismate pathway in yeast.

The structure of Aro1 itself also shows evidence of co-functionality between the domains. The protein acts as a homo-dimer and each monomer can be structurally divided into two parts;

one containing the DHQ synthase and the 5-ESP synthase domains and the other half containing the shikimate kinase, DHQase and the shikimate dehydrogenase domains⁴⁵ (Figure 4). It has been shown that the different domains of the pentafunctional protein have intrinsic interactions with the others that affect the catalytic functionality of the domains. This is especially true of the DHQ synthase and the 5-ESP synthase domain containing half of the

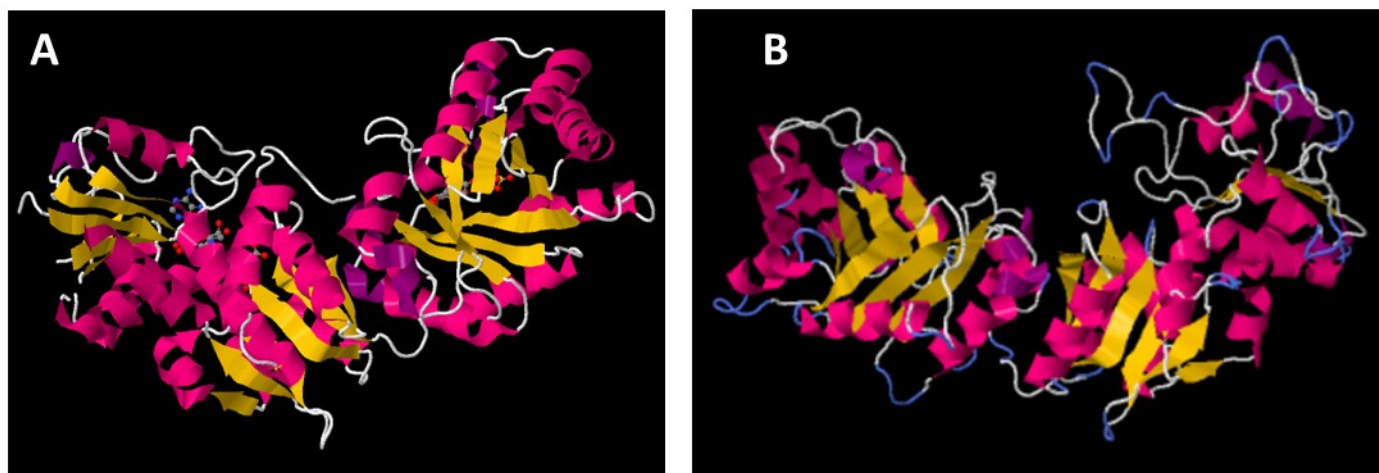


Figure 3. Comparison of *A. thaliana* DHQ-SDH protein and homologous domains of *S. cerevisiae* Aro1

A) Model of the *A. thaliana* DHQ-SDH protein. The model was generated using the crystal structure published by Singh *et al.*⁸⁶ The 3-dehydroquinase (DHQ) domain is on the left and the shikimate dehydrogenase (SDH) domain is on the right. The protein shows a concave structure that has been demonstrated to facilitate metabolic channeling by increasing the local concentrations of substrates. **B)** Structure of *S. cerevisiae* Aro1 from residues 1078 - 1587. The model was built using the Phyre2 modeling platform and has a structural alignment at a 100% confidence with the *A. thaliana* DHQ-SDH protein. The DHQ domain is on the left and the SDH domain is on the right. The two domains form a concave shape similar to the *A. thaliana* DHQ-SDH, possibly for the same function.

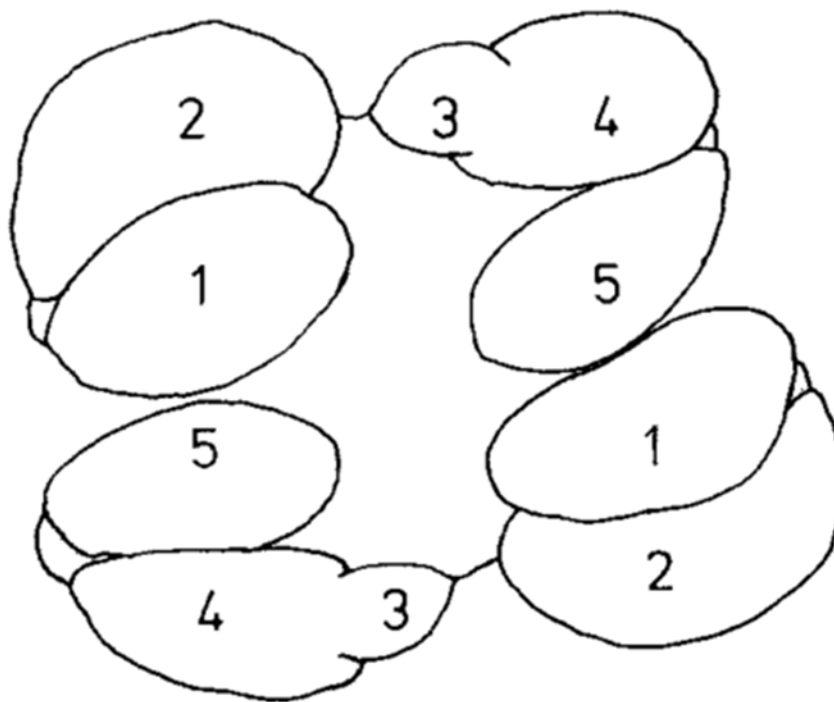


Figure 4. Representation of internal structure of *S. cerevisiae* Aro1 homo-dimer. The domains are 1: DHQ synthase; 2: 5-EPS synthase; 3: shikimate kinase; 4: DHQase; 5: shikimate dehydrogenase⁴⁵. The dimerization interface is between domains 1 and 5.

protein. Multiple deletion and co-expression studies have demonstrated that the 3-ESP synthase domain's catalytic functionality is directly dependent on its *cis* bonding to structurally complete DHQ synthase domain⁸⁶. If the DHQ synthase domain is replaced by another folded

protein or not present in its entirety there is complete abatement of 5-ESP synthase activity. Similarly, the DHQase domain and the shikimate dehydrogenase domain are the dimerization interface for the AroM homo-dimer⁴⁵. Thus, the deletion of the shikimate dehydrogenase domain would destabilize the dimerization of Aro1 and would have a detrimental effect on the functionality of the Aro1 complex as a whole and negatively affect the flux going through this pathway⁹⁰.

Taking all this into account we can surmise that the *S. cerevisiae* Aro1 protein probably does not have very high substrate channeling activity, although it does produce enzyme co-localization to increase flux through the chorismate pathway. The flux through the chorismate pathway can be up-regulated by removing the feedback inhibition acting on the DHAP synthase and separately over-expressing the AroB and AroD domains. Additionally, any major deletion in the Aro1 catalytic domains will change the structure of the Aro1 enzyme and negatively affect the flux going through it and may even ablate its activity completely.

Therefore, to increase the accumulation of DHS for increasing the flux towards CCM production, four different strategies were considered (Figure 5). I hypothesized that the deletion of the entire Aro1 protein or modulation of the shikimate dehydrogenase active site or decreasing the expression level of the Aro1 protein will lead to an accumulation of DHS which will subsequently lead to higher carbon flux to PCA and the heterologous CCM pathway.

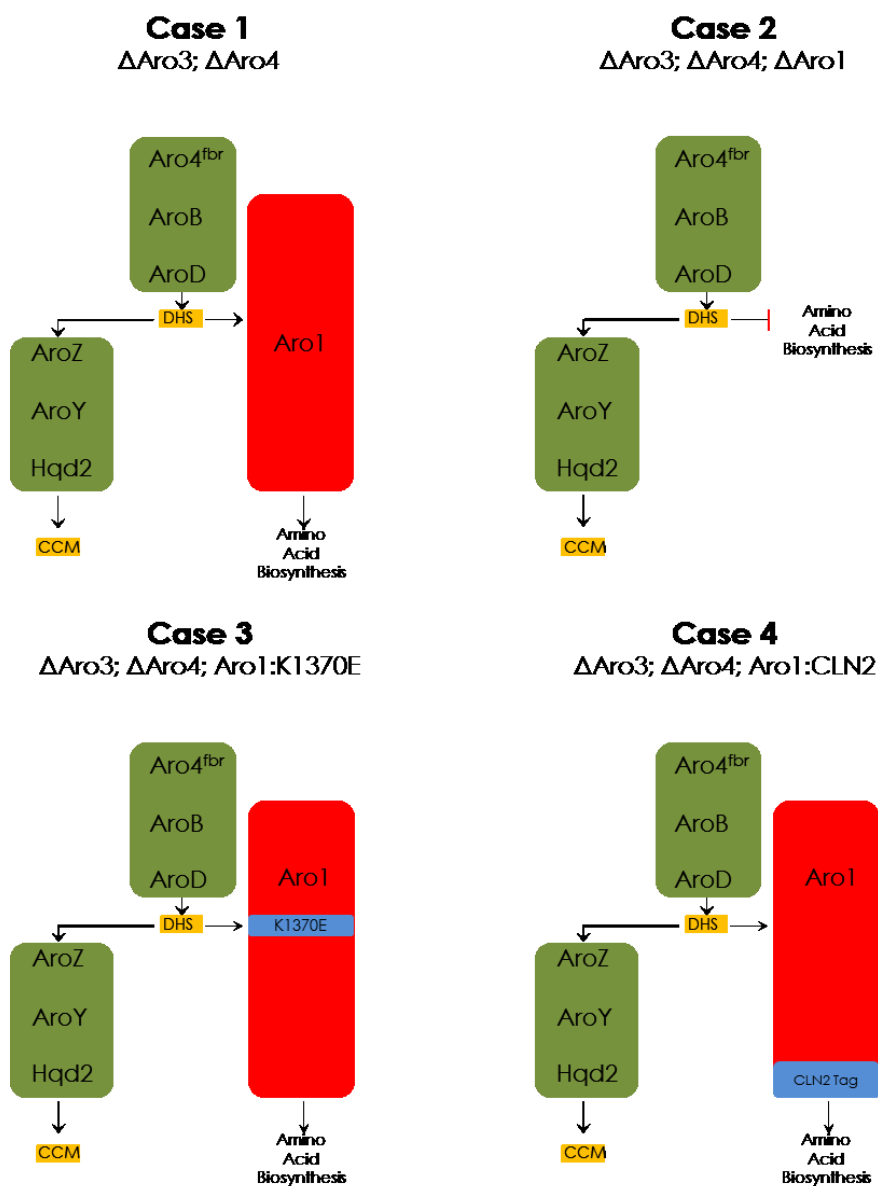


Figure 5. Representations of experimental plan for this study. The optimization of DHS accumulation in order to channel more carbon into the heterologous *cis,cis*-muconic acid pathway will be explored in four cases. The desired flow of carbon through the cell is shaded in green; the native Aro1 protein is shaded in red and represents the unwanted siphoning of DHS into native metabolism. Any modifications to Aro1 are designated in blue. **1)** The chorismate pathway will be completely deregulated by deleting the native DAHP synthases, *aro3* and *aro4*, and over-expressing a feedback inhibition resistant mutant *aro4*^{K229L}. Additionally, the *E. coli* genes *aroB* and *aroD* will be expressed to overcome previously identified bottlenecks to DHS production. **2)** *aro1* will be deleted in the previously described strain to prevent loss of DHS to the native metabolic pathway in an attempt to increase CCM production. **3)** The shikimate dehydrogenase domain of Aro1 will be mutated in the strain from Case 1 to greatly reduce conversion of DHS into shikimate. **4)** Aro1 from strain one will be tagged with a rapid-degradation tag in order to reduce its abundance in the cell with the intention of decrease its ability to siphon DHS into the native aromatic molecule pathway

1.4 Rationale and Proposed Metabolic Engineering Objectives

1.4.1 Deletion of *Aro1* to Increase Accumulation of 3-Dehydroshikimate

Aro1 is a critical enzyme in the shikimate pathway that produces precursors for all aromatic amino acids and a large number of aromatic vitamins such as Vitamin B12, folate and *p*-aminobenzoic acid (PABA), which are essential for growth. Removing its functionality from the cell's metabolism has been shown to cripple the cells and to have a large negative effect on their growth^{67,91}. Therefore, the growth conditions that would be feasible to grow an *aro1* null deletion strain of *S. cerevisiae* will be explored using the *S. cerevisiae* deletion strain collection⁹². These deletion strains are based on the common laboratory strain BY4741 and are auxotrophic for histidine, leucine, methionine and uracil. These amino acids will be supplemented in the growth media to complement the auxotrophies. As the chorismate pathway is the precursor pathway to produce all the aromatic amino acids, ostensibly, supplementing the media with certain amounts of aromatic amino acids might rescue the growth phenotype in an *aro1* null deletion. However, supplementing an industrial production strain with amino acids or growing the strain in rich media gets cost-prohibitive at larger scales, thus the resulting Δ *aro1* strain will also be evolutionarily adapted to minimize aromatic supplementation. Adaptive evolution takes advantage of selective pressure and the *S. cerevisiae*'s high DNA recombination frequency and modularity in gene expression levels to select for user-defined traits in the chosen organism⁹³⁻⁹⁵. Thus the Δ *aro1* strain will be grown with decreasing amounts of aromatic molecule supplementation in the growth media until the minimal amount of supplementation for viable and robust growth is determined. This method would be the most effective way to remove shikimate production in the cell and direct all the carbon into the heterologous pathway.

1.4.2 Mutating *aro1* to Remove Shikimate Dehydrogenase Functionality to Accumulate 3-Dehydroshikimate

To avoid the drastic metabolic effect of deleting Aro1's functionality, a more elegant solution would be to minimize and limit the conversion of DHS to shikimate to only what is minimally required for cell viability. This can be achieved by mutating the shikimate dehydrogenase active site in Aro1 to decrease its catalytic efficiency. The shikimate dehydrogenase domain of *S. cerevisiae* Aro1 has not been analyzed by mutation analysis. However, multiple homologs of prokaryotic shikimate dehydrogenases have been crystallized and their active sites determined⁹⁶⁻⁹⁹. The active site is divided into two domains, the NADPH binding domain and the catalytic domain⁹⁹. There are multiple highly conserved residues throughout the protein, mostly in the NADPH binding module. However, there is a highly conserved lysine (K) residue in the substrate binding/catalytic module that has been computationally implicated in the binding of DHS⁹⁸ (Figure 6). The positively charged lysine residue at the opening of the active site is hypothesized to stabilize the binding of DHS to the active site. Modifying this residue into one that has a neutral or opposite charge would disrupt its stabilizing effect and reduce the efficiency of DHS binding to the active site. This lysine residue has also been targeted for mutagenesis in the *A. thaliana* bi-functional DHQ-SDH protein⁸⁷. Mutating this residue to a negatively charged aspartic acid showed a strongly decreased shikimate dehydrogenase activity *in vitro*. The decreased binding stability of DHS to Aro1 would decrease the catalytic efficiency of the Aro1 shikimate dehydrogenase domain, which would subsequently lead to decreased shikimate production and an increased accumulation of DHS in the cell.

1.4.3 Reducing the Abundance of Aro1 to Increase 3-dehydroshikimate Accumulation

Decreasing the abundance of a protein decreases the total amount of substrate converted into the product by the protein. The expression level of the protein and its rate of degradation determine its cellular abundance. The expression level of a protein is mostly determined by its native promoter strength and by transcription factor regulation which can affect the rate and

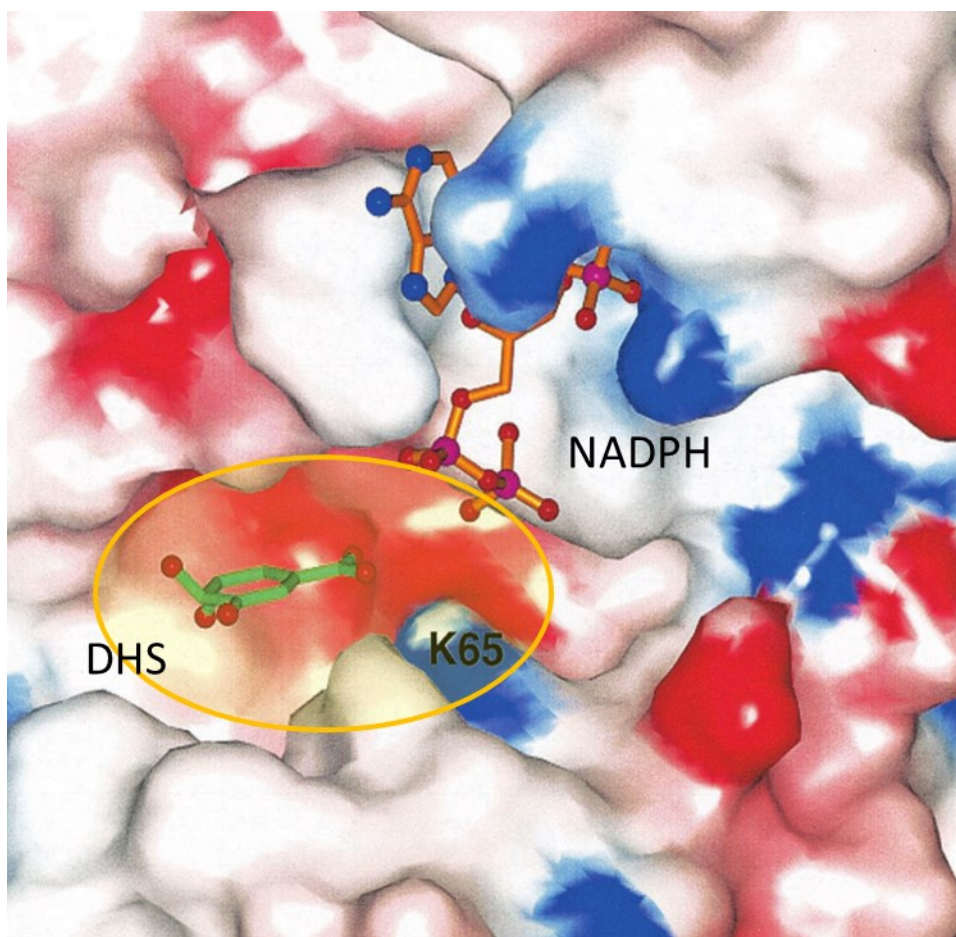


Figure 6. Model of the *Haemophilus influenzae* AroE shikimate dehydrogenase active site. This protein has a nearly identical structure to the *S. cerevisiae* shikimate dehydrogenase domain as it is highly conserved⁹². Positive charges are colored in blue while negative charges are in red. The proposed 3-Dehydroshikimate (DHS) binding pocket is highlighted in yellow. The positively charged lysine residue marked in the binding pocket stabilizes the interaction between the carboxylic acid group of DHS and NADPH for the reaction to occur. Disruption of this stabilizing function has been shown to decrease the interaction between the enzyme, DHS and NADPH, reducing the amount of DHS that is converted to shikimate.

timing of the protein's expression¹⁰⁰. Degradation of a protein can be affected by adding specific degradation tags on the protein, which hasten or delay the degradation process¹⁰¹. *S. cerevisiae*, like all other organisms has a tightly controlled cell cycle. The proteins that regulate entry and exit to and from each cell cycle, cyclins, must be expressed and degraded very rapidly to prevent overlapping cell cycles that can be deadly to the cell¹⁰². Most of the cyclins have a specific domain that targets the protein for degradation via the ubiquitin system^{103,104}. Cyclins that mediate the G1 to S transitions in the cell have a particular degradation domain rich in proline, glutamine, serine and threonine (PEST domains) that specifically target the proteins for degradation via the constitutive ubiquitin pathway¹⁰⁵. The PEST degradation domain from Cln2p has been used to tag GFP and the complete ablation of the GFP signal was observed 30 minutes after inoculation¹⁰⁶. Thus, this domain will be inserted on the N' terminal of Aro1 to dramatically reduce its cellular abundance and subsequently increase the cellular accumulation of DHS.

2. MATERIALS AND METHODS

2.1 Strain and Plasmid Construction

2.1.1 Construction of Plasmid Expressing Recombinant CCM Pathway

All strains and plasmids used in this study are reported in Table 1. All plasmids were assembled using overlapping DNA parts and transformation assisted recombination in yeast¹⁰². All PCR amplifications of the DNA parts were done using primers listed in Table 2 and Phusion HF Polymerase (ThermoFisher F-530S) according to the manufacture's recommended protocols. The gene encoding the Aro4^{K229L} feedback resistant variant was amplified by PCR from a previously created point mutation of *aro4^{fbr}* as described by Luttick *et al*⁴⁹. The *aroB* and *aroD* genes were amplified from wild-type DH5 α *E. coli* genomic DNA. The 4BD plasmid (p4BD) was based on the pYES high-copy plasmid system¹⁰³. The 3-dehydroshikimic dehydratase, *aroY* from *P. anserina*; the protocatechuic acid decarboxylase, *aroZ* from *K. pneumoniae*; and the catechol-

Table 1. Plasmids and strains used in this study and their corresponding genotypes

Plasmid	Origin Vector, Auxotrophy	Description	Reference
EV	pYES2, URA3	No genes inserted	103
4BD	pYES2, URA3	<i>tef1_p-aro4^{K229L}-pgi_{ter}; pgk_p-aroB-adh1_{ter} and tdh3_p-aroD-adh2_{ter} from E. coli</i>	This study
DAC	pGREG506, URA3	<i>Pdc1_p-aroZ-eno2_{ter} from P. anserina; fba1_p-aroY-tpi_{ter} from K. pneumoniae; pma1_p-hqd2-cyc_{ter} from C. albicans</i>	This study
6g	pGREG506, URA3	<i>tef1_p-aro4^{K229L}-pgi_{ter}; pgk_p-aroB-adh1_{ter} and tdh3_p-aroD-adh2_{ter} from E. coli; Pdc1_p-aroZ-eno2_{ter} from P. anserina; fba1_p-aroY-tpi_{ter} from K. pneumoniae; pma1_p-hqd2-cyc_{ter} from C. albicans</i>	This study
pSH47	URA3	CRE-recombinase under Gal1 promoter	107

Strain	Genotype	Plasmid	Parent Strain	Reference
BY4741	MAT a; <i>his3Δ1 leu2Δ0 met15Δ0 ura3Δ0</i>	None	S288C	91
BY4741 <i>aro1</i>	MAT a; <i>his3Δ1 leu2Δ0 met15Δ0 ura3Δ0 aro1</i>	None	BY4741	91
13D		None	<i>S. cerevisiae</i>	105
13DpEV		EV	CEN.PK 113	
13p4BD	Mat α; <i>MAL2-8c; SUC2; ura3-52</i>	4BD	13D	
13DpDAC		DAC		
13Dp6g		6g		
K34		None	<i>S. cerevisiae</i>	This study
K34pEV	Mat α; <i>MAL2-8c; SUC2; ura3-52;</i>	EV	CEN.PK 113	
K34p4BD	<i>aro3; aro4</i>	4BD	13D	
K34p6g		6g		
K341		None	K34	This study
K341pEV	Mat α; <i>MAL2-8c; SUC2; ura3-52;</i>	EV		
K341p4BD	<i>aro3; aro4; aro1</i>	4BD		
K341p6g		6g		
K34M		None	K34	This study
K34MpEV	Mat α; <i>MAL2-8c; SUC2; ura3-52;</i>	EV		
K34Mp4BD	<i>aro3; aro4; ARO1^{K1370E}</i>	4BD		
K34Mp6g		6g		
K34A1Cln2	Mat α; <i>MAL2-8c; SUC2; ura3-52;</i>	None	K34	This study

K34 A1Cln2pEV	<i>aro3; aro4; ARO1-CLN2_{PEST}</i>	EV
K34 A1Cln2p4BD		4BD
K34 A1Cln2p6g		6g

Table 2. Primers and other guide-RNA sequences used in this study

Primer Description	Primer sequence (5' – 3')
Kanamycin resistance cassette for <i>aro4</i> deletion	FWD: atgagtgaatctccaatgttcgctgccaacggcatgccaaggtaaatacagctgaagcttcgtacgctgcagg REV: ctatttcttgtaacttctctctttgtctgacagcagcagccaattccggccgcataggccactagtggatctg
Hygromycin resistance cassette for <i>aro3</i> deletion	FWD: atgttcattaaaaacgatcacgccggtgacaggaaacgcttggaagactgcagctgaagcttcgtacgctg REV: ctatttttcaaggcctttctctgtttctaacaccttgcgaatagctggccgcataggccactagt
Kanamycin resistance cassette for <i>aro1</i> deletion	FWD: atgggtgcagttagccaaagtccaattctaggaatgatattatccacgtcagctgaagcttcgtacgcg REV: ctactcttcgtaacggcatcaaaaatggccttgaaagggccttgaaatcgccgcataggccactagt
<i>aro4^{fbr}</i>	<u><i>tef1_p</i></u> p4BD_FWD: aggaataactctgaataaaacaacttataataaaaaatgcatagcttcaaaatgtttctactc p6g_FWD1: gagactgcagcattactttgagaagatagcttcaaaatgtttctactcctttttac p6g_FWD2:tcactaaagggaaacaaaagctggagctcgtttaaacggcgccgagactgcagcattactttgagaag REV: tgtttaattatttctctcttttataataaattttctagattaaaacttagattagattgctatg
	<u><i>aro4^{fbr}</i></u> FWD:ctagaaaatttattataaaaaggaagagaaataattaacaatgagtgaatctccaatgttcg REV: aaagtctattattaattgggtgtgtttcagttttatgtctctatttctgttctctctttgtc
	<u><i>pqi_{ter}</i></u> FWD: agacataaaaactgaaacaacaccaattaataatagactttaacaaatcgctcttaaatatatac REV: catctgtccacttgatgtttatgcgttttctaagaccgggtatactggaggcttcat
	<u><i>pqk1_p</i></u> FWD: ccggtcttagaaaacgcataaacataacaagtgacagatgacgcacagatattataacatct REV: tgtttaattagtaattgttggtgtgactggtagatgtgttatactggaggcttcatgattatgtcc
<i>aroB</i>	<u><i>aroB</i></u> FWD: ctagaaaatttattataaaaaggaagagaaataattaacaatggagaggattgtcgttactc REV: aaagtctattattaattgggtgtgtttcagttttatgtctttacgctgattgacaatcggc
<i>aroD</i>	<u><i>adh1_{ter}</i></u> FWD: taataattaataactattttcaaaattctacttaaaaataggacttcttcgcca REV: tgattgtaagaatgtttagtgatgagtatgttatttaaggcatgccggtagag
	<u><i>tdh3_p</i></u> FWD: cttaaataacatactcatcactaaacattcttaacaatcatcgatttatcattatcaact REV: tgtttatttaatttaattatgatatgtttatgggatgtcgaaactaagtcttgggt
	<u><i>aroD</i></u> FWD: ctagaaaatttattataaaaaggaagagaaataattaacaatgaaaaccgtaactgtaaaaga REV: aaagtctattattaattgggtgtgtttcagttttatgtctttatgctgtgtaaaatagttaatacc
	<u><i>adh2_{ter}</i></u>

FWD: tataataagattccataataaaattaataaataataatctgcgatctcttatgtcttt
p4BD_REV: tgttaattagtaattgttggctgttgactggtatgtggtatactggaggcttcatgagttatgtcc
p6g_REV: gcattttattatataagttgtttattcagagtattccttagaattataaacttgatgagatgag

pdC1_p

pDAC_FWD: aggaataactctgaataaaacaacttatataataaaaatgcacatgcgactgggt
p6g_FWD: attgcgaagactatactgatatgaatttaaactagagcacatgcgactgggt
REV: tgttaattatttctctcttttataataaatttctagattaaacttagattagattgctatg

aroZ

aroZ

FWD: catccatataaacatatcataaattaataaataaacaacatgcgactgggtgagcatatgttccg
REV: agattattatttataattttattatggaatcttattataaggtatcatctccatctccc

eno2_{ter}

FWD: agcagcccatcaggatgctgtcgtgtcagcggcttgtaaagtgttttaactaagaattattagcttttctgc
REV: aaggctggattgttcaagccagcgggtccagttggataggtatcatctccatctcccatatgc

fbA1_p

FWD: gaccacagtgatgcatatgggagatggagatgatacctatccaactggcaccgctggc
REV: gcgcgatggcgtcgcgagatcctgaatcggtgcggtcattatgtattacttggttatggttatatgac

aroY

aroY

FWD: acatctaccagtcaacagccaacaattaactaattaacaatgaccgcccattccaagattg
REV: tatttttaagtagaattttgaaaatagatttaattattacttggcggaaccttgattctttcc

tpi_{ter}

FWD: tttcgccggctggaaaaaaaccagggtagcgaataaagattaatataattatataaaaatattatcttc
REV: caaaacagagtgatgtatgggtgatccagcaatgcctgtctatataacagttgaaattgaaataagaac

pma1_p

FWD: ttgagaagatgttcttattcaaatttcaactgttatatagacaggcattgctgggatcacc
REV: cctaaggaggttttaacactttcagtaaaagctgtgacattttgataaataatctttctatc

Hqd2

hqd2

FWD: catccatataaacatatcataaattaataaataaacaatgtccaagccttcaccgaatctg
REV: agattattatttataattttattatggaatcttattatattacaacttgattcagcatctgtctagc

cyc_{ter}

FWD: tgccccaaggcaagacaagatgctgaaattaattgtaatcatgtaattagttatgtcacgc
pDAC_REV: tgttataattattttcttattttgatgtaataaagagggcaaattaagccttcg
p6g_REV1: gtatgctatacgaagttattaggtaccgcgccgcgcaataaagccttcgagcgtccc
p6g_REV2: ataacttctataatgtatgctatacgaagtattaggtaccgcgccgcacaactcatggtgatgag

Vector backbone

FWD: cctcttatattacatcaaaaataagaaaataattataaacctgcattaatgaatcggccaacgcgccccg
REV: gcattttattatataagttgtttattcagagtattctgccttagcgccttaagcgcgg

Cas9 Plasmid

Cas9 part

FWD: aggaataactctgaataaaacaacttatataataaaaatgcatagcttcaaatgttttactcctttttactc
REV: catctgtccactgtatgtttatgcgttttctaagaccgggcaaattaagccttcgagcg

gRNA part

FWD: ccggtcttagaaaacgcataaacatacaagtgacagatgtctttgaaaagataatgtatgattatgcttcc
REV: tgttataattattttcttattttgatgtaataaagaggtatccactagacagaagtttgcgttcc

gRNA targeting region for Round 1

attggtgaaagaaaacttt

Aro1 Mutagenesis

FWD: attggtgaaagaaaactttgttttagagctagaatagc
REV: aaagttttctttcaccatgatcatctttctcactgccc

Stuffer region sequence and targeting qRNA sequence

agatgcgggagaggttctcg

FWD: agatgcgggagaggttctcggttttagagctagaaatagc

REV: cgagaacctctcccgcacatctgatcatttatctttcactgc

Inserting aro1 region into plasmid for mutagenesis

FWD: aggaataactctgaataaaaacaacttatataataaaaatgcggttcccatgacttcc

REV: tgttataattattttctattttgatgtaataaaagaggaataaggttggtacaaaagcagc

Mutagenesis primers

FWD: ctctggaattagacataatgcagtagatgatgaattgactgatgc

REV: ggcgattcagaatggccaattggcttccaacaacaacagttcc

Primers for re-insertion of mutagenized fragment

FWD: tactcctgggacgacgc

REV: ctgacagcaacgccaacg

qRNA targeting region

agcattgtaaaatataaaaa

FWD: attggtgaaagaaaaactttgttttagagctagaaatagc

REV: aaagttttctttcaccaatgatcatttatctttcactgcgg

50bp aro1- cln2_{PEST} – 50bp aro1

FWD: ttgatgccgtgacaaaggaagcatccaactgaacatttcgagaaagc

REV: gcattgtaaaatataaaaaaggatagatatattgtctatattactgggtattgcc

Aro1-Cln2_{PEST}

500bp aro1 homology on 5' of cln2_{PEST} domain

FWD: gttatcgggtgcaggtggcacttc

REV: gaaatgttcaagttggatgcttctttgtcacggcatcaaaaatggccttg

500bp aro1 homology on 3' of cln2_{PEST} domain

FWD: tttttatattttacaatgcttctatgatatctttactaagatgagttgcc

REV: cggaccttcatttatactactgc

1,2-dioxygenase, *hqd2* from *C. albicans* were codon-optimized and synthesized by GeneArt, (Life Technologies Incorporated, Burlington, ON). These genes were further sub-cloned individually and in combination with *aro4^{fab}*, *aroB*, *aroD* into single copy CEN/ARS based pGREG plasmids¹⁰⁴ to test functionality. DNA was transformed into *S. cerevisiae* CEN.PK 13D¹⁰⁵ strains using the lithium acetate heat shock method as described by Gietz *et al*¹⁰⁶.

2.1.2 Yeast Genes Deletion

Aro4 and *aro3* were deleted in complementary mat-a and mat- α strains using homologous recombination and selection on 200 μ g/ml of G418 and hygromycin, respectively as previously described¹⁰⁷. Isolated colonies under antibiotic selection were picked and the presence of the deletion was confirmed by PCR on extracted genomic DNA. The cognate mat-a and mat- α strains were then plated on the same YPD plate and left to mate overnight at 30°C. The mated cells were streaked to isolate single colonies and diploid cells were identified based on size and shape using a light microscope. These diploid cells were streaked on pre-sporulation media (Bacto-Yeast Extract 8 g/L, Bacto-Peptone 3 g/L, Dextrose 100 g/L, Agar 20 g/L) followed by sporulation media (Potassium Acetate 10 g/L, Bacto-Yeast Extract 1 g/L, Dextrose 500 mg/L, Agar 20 g/L) for 4 days each in order to recover haploid cells¹⁰⁸. These cells were confirmed to be haploids by their size and shape under the light microscope and by performing a mating test with known haploid strains. The confirmed haploids cells were selected on YPD plates containing both G418 and hygromycin to select for both *aro3* and *aro4* deletions. Isolated colonies under antibiotic selection were selected and the presence of both the deletions was confirmed by PCR on extracted genomic DNA. The double deletion strain was cured of the loxP-flanked antibiotic selection cassettes using a Cre recombinase and replica plating was used to identify colonies with no antibiotic resistance. The cured double deletion strain *S. cerevisiae* CEN.PK 13D *ura3 aro4 aro3* was named K34. Strain K34 was used as a base strain to create all other strains used in this study. The *aro1* deletion was made and selected for using the same LoxP-flanked G418-selection based homologous recombination cassette. The resulting strain, *S. cerevisiae* CEN.PK 13D *ura3 aro4 aro3 aro1*, was verified using PCR on extracted genomic DNA and named K341 (Table 1).

2.1.3 Modification of Chromosomally Encoded Aro1

The *Aro1*^{K1372E} point mutant was created in a two-step process (Figure 7). The shikimate dehydrogenase domain active site of the *aro1* coding region was amplified by PCR and inserted into a pYES vector using the Gibson assembly method¹⁰⁹. Site-directed mutagenesis (SDM) of the selected active site region was performed using a QuickChange protocol (ThermoFisher) and the primers listed in Table 2. The resulting plasmid containing the modified active site was transformed into *E. coli* and subsequently sequenced to confirm the location of the point mutation. To facilitate a scar-less insertion of the modified active site back into the native *aro1* coding region, two rounds of CRISPR-based recombination¹¹⁰ were used. Firstly, a 20-bp non-native stretch of DNA (stuffer region) was inserted into the target region of *aro1* of strain K34 (see Table 2 for gRNA and stuffer sequence used). The point mutant version of the active site DNA fragment previously created by SDM was then amplified by PCR and used as a donor in a second round of CRISPR, targeting the non-native stuffer region as the cleavage site. The chromosomally-encoded modified shikimate dehydrogenase domain was amplified by PCR from several clones and sequenced to confirm the presence of the mutation. This resulted in a scar-less insertion of a mutation of *aro1* in a K34 based strain. This strain, *S. cerevisiae* CEN.PK 13D *ura3 aro4 aro3 aro1*^{K1370E}, was named K34M.

The Cln2 tag was inserted at the 3' end of *aro1* to act as a rapid degradation tag¹⁰¹. The piece of DNA to be inserted into the chromosome was created in three parts. The PEST domain from *cln2* was amplified with 50 bp homology to the 3' end of *aro1* on either side of the domain. Additionally, two 500 bp regions from the 3' of *aro1* were amplified to overlap the 50bp of *aro1* homology on the PEST domain. (See Table 2 for primers used) DNA soeing (splicing by overlap extension) using PCR amplification was subsequently used to combine the three pieces of DNA to create one piece of DNA containing the *cln2* PEST domain flanked by 500 bp of homology to the 3' end of *aro1* on either side. This piece of DNA was then used as a donor in a CRISPR-assisted insertion targeting the 3' region of *aro1*. Several isolated colonies were picked and correct insertion of the Cln2 tag was confirmed by PCR amplification of the genomic region followed by sequencing.

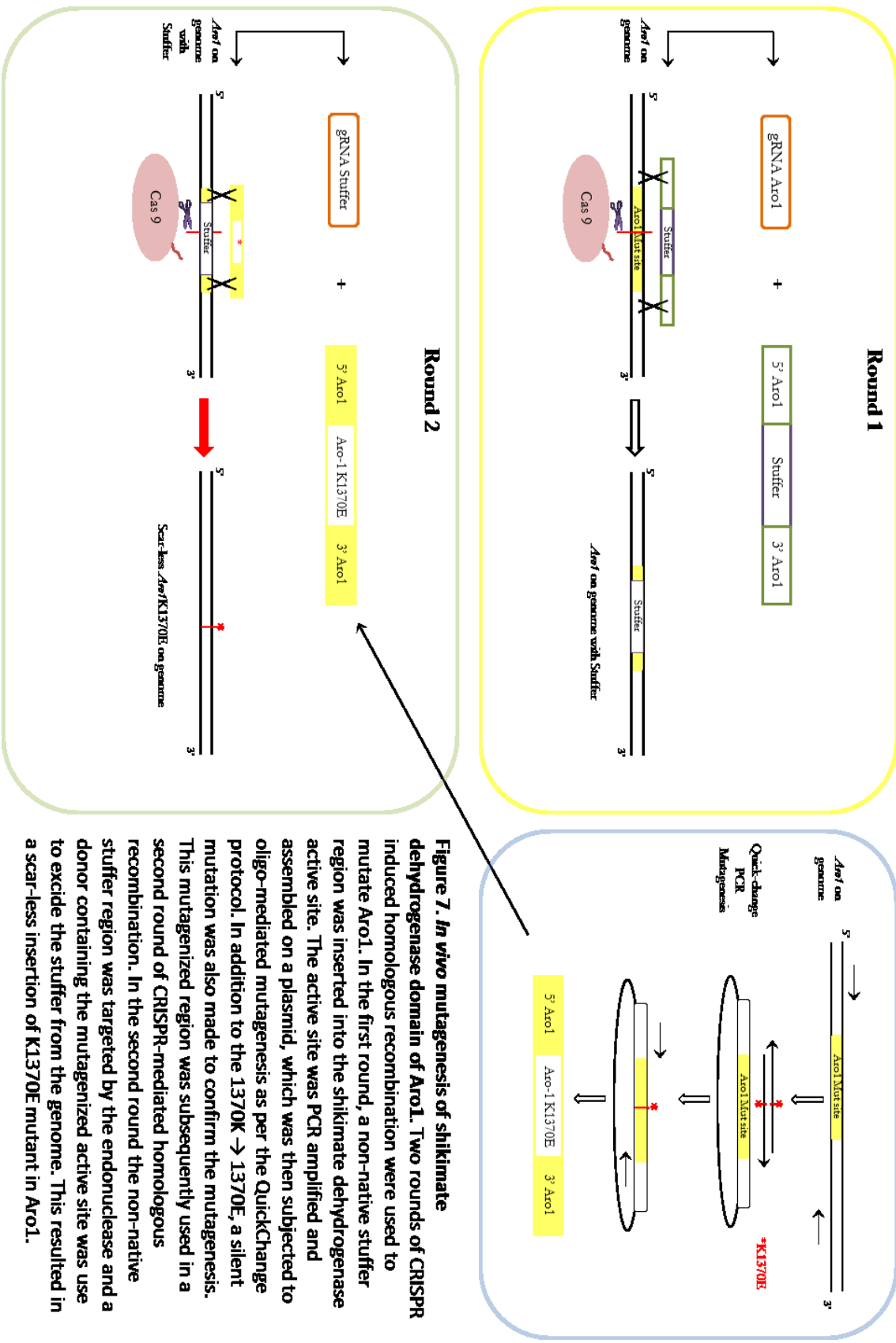


Figure 7. *In vivo* mutagenesis of shikimate dehydrogenase domain of Aro1. Two rounds of CRISPR induced homologous recombination were used to mutate Aro1. In the first round, a non-native stuffer region was inserted into the shikimate dehydrogenase active site. The active site was PCR amplified and assembled on a plasmid, which was then subjected to oligo-mediated mutagenesis as per the QuickChange protocol. In addition to the 1370K → 1370E, a silent mutation was also made to confirm the mutagenesis. This mutagenized region was subsequently used in a second round of CRISPR-mediated homologous recombination. In the second round the non-native stuffer region was targeted by the endonuclease and a donor containing the mutagenized active site was used to excise the stuffer from the genome. This resulted in a scar-less insertion of K1370E mutant in Aro1.

The resulting strain, *S. cerevisiae* CEN.PK 13D *ura3 aro4 aro3 aro1-cln2_{PEST}* was named K34A1Cln2.

2.2 Strain Growth and Fermentation Conditions

All reagents were purchased from Sigma Aldrich Canada unless specifically mentioned. YPD medium (broth or 1% (w/v) agar plates) was used for antibiotic selection. Growth for testing of the strains for metabolite production was done in 25-ml shake flasks with YNB + 0.25 X Dropout medium + 2% (w/v) glucose + 35 mg/L tryptophan. All strains were inoculated into testing media from stationary phase overnight cultures at a 5% (v/v) inoculum. Testing of the viable growth conditions of the *aro1* deletion K341 strain was performed in 25 ml of YNB + 2% glucose + 1X vitamin mix (biotin 2 µg/L, calcium pantothenate 400 µg/L, folic acid 2 µg/L, inositol 2 mg/L, nicotinic acid 400 µg/L, *p*-aminobenzoic acid 200 µg/L, pyridoxine HCl 400 µg/L, riboflavin 200 µg/L and thiamine HCL 400 µg/L) and varying concentrations of dropout media; 3X, 2X, 1X, 0.5X, 0.25X and no dropout media. All O.D. readings were performed using a Cary 50 (Agilent Technologies Mississauga, ON) at 600nm.

Two-step fermentation with different growth media at each step was performed similar to the methodology described by Horwitz *et al*⁹⁰. Strain K341 p6g (Table 1) was inoculated from a stationary phase culture into 25 ml of YPD broth in 250 ml erlenmeyer flasks and incubated at 30°C and 250 RPM for 48 hours. The cells were pelleted at 4000 X g for 5 minutes and washed twice in 10 ml of deionized water. The cells were subsequently added to 25 ml of YNB + 4% glucose and incubated at 30°C and 250 RPM for a further 72 hours. O.D. 600 readings and samples were taken at regular intervals to quantify metabolite accumulation.

Anaerobic cultures were first grown under aerobic conditions for 36 hours at 30°C. At 36 hours, 1 ml of 25 mg/ml glucose was added to the cultures and the headspace was replaced with nitrogen gas. These cultures were subsequently sealed with Parafilm and aluminum foil, capped tightly and incubated at 30°C and 250 RPM for 48 hours. The caps and the seal were then removed and the strains were allowed to ferment aerobically for 36 more hours. O.D. readings and samples for metabolite quantifications were taken at regular intervals.

2.3 Metabolite Identification and Analysis

All metabolite were measured from the culture supernatants. For preparation of samples to be analyzed, 300 μL of cell culture was collected and 250 μL of the supernatant was retained after centrifugation at 13000 X g for 5 minutes. The supernatants were subsequently filtered using nitrocellulose syringe filters (Cole-Parmer, RK-02915-53) to remove cell mass and debris. Twenty μL of supernatant was injected per analysis. The metabolites were identified using HPLC equipped with a UV/Vis detector (Thermo Surveyor) and a Waters 3100 refractive index detector. A Bio-Rad ion exchange column Aminex HPX-87H was used with 10 mM sulphuric acid as an isocratic mobile phase with a flow rate of 0.6 mL/min. Shikimate, DHS, pyruvate, acetate, protocatechuic acid, catechol and CCM were analyzed using a UV/Vis detector at standard wavelengths of 210 and 280 nm. Glucose and ethanol were measured using their refractive index. All measurements were compared to linear standard curves of reference standards.

3. RESULTS

3.1 Removing Feed-back Inhibition in the Chorismate Pathway

The first step in the over-accumulation of DHS was to maximize the carbon flux entering the chorismate pathway. The pathway is feedback-inhibited by its downstream products, tyrosine and phenylalanine. At cellular concentrations above basal metabolic levels tyrosine and phenylalanine inhibit the activity of Aro3 and Aro4, limiting the amount of carbon entering the chorismate pathway⁴¹. This was overcome by the deletion of the native feedback-inhibited DAHP synthases, *aro3* and *aro4*, as previously described by Luttick *et al.*⁴⁹ and overexpression of the feedback-resistant Aro4^{K229L} mutant. The accumulation of DHQ has also been previously identified as the second bottleneck in the early chorismate pathway⁵². To this effect, a plasmid, p4BD, expressing a feedback resistant Aro4 (Aro4^{fbr}), AroB and AroD was transformed into the wild-type and feed-back resistant strains. Upon growth on minimal media, the feedback-resistant strain harboring the p4BD plasmid (Strain K34 p4BD, Table 1), accumulated $369.9 \pm$

22mg/L of shikimic acid (Figure 8D) as compared to the wild-type strain (Strain 13D pEV), which only accumulated 13.1 ± 1 mg/L of shikimic acid demonstrating the effectiveness of the engineered pathway. Strain K34 p4BD also accumulated 28.3 ± 1.9 mg/L of DHS representing a 2-fold improvement over the wild-type strain over-expressing p4BD (13D p4BD, Table 1) (Figure 8C). Strain 13D pEV shows much slower growth rate and glucose consumption rate as compared to the other strains; this is an artifact caused by a smaller starting concentration of cells (Figure 8A & 8B). The large accumulation of shikimic acid suggests that Aro1 was converting the accumulated DHS into downstream precursors of the chorismate pathway. Thus, the Aro1 node needs to be modulated to prevent accumulation of shikimic acid. This can be done in three ways; the entire *aro1* gene could be deleted from the strain ablating the encoded functionality completely; the shikimate dehydrogenase domain of Aro1 can be targeted for mutagenesis to effectively and precisely knock out its functionality; and the abundance of the entire Aro1 protein in the cell can be diminished to reduce its effectiveness at converting DHS to shikimic acid.

3.2 Deletion of Aro1 and its Effect on DHS Accumulation

The deletion of Aro1 functionality from the cell should remove DHS utilization for cellular metabolism and lead to its accumulation as shown by Horwitz *et al.*⁹¹. As Aro1 is essential in the chorismate pathway and produces precursors that lead to all aromatic molecule production in the cell, its deletion could have adverse effects on the growth of the cell. The Yeast Deletion Library⁹² was used to test the feasibility of creating a strain with no Aro1 functionality. The BY4741 Δ *aro1* strain was grown in synthetic complete (SC) media with the different aromatic amino acids as sole aromatic molecule sources (Table 3). The amino acid supplement contained 76 mg/L of tyrosine and phenylalanine and was used as a baseline to screen the aromatic molecule supplements. The growth phenotype of the Δ *aro1* strain was not rescued by the presence of 76 mg/L of phenylalanine and tyrosine in the growth media.

Table 3. Investigation of growth conditions of $\Delta aro1$ *S. cerevisiae* strains. # represents the number of colonies observed on the plate.

CONDITIONS		STRAIN	Y/N (#)
YPD		BY 4741 Δ Aro1	Y
YNB Δ a.a DO (Synthetic complete Drop-out) +2% Glucose		BY 4741	N
YNB Δ a.a DO +2% Glucose		BY 4741 Δ Aro1	N
YNB + a.a DO +2% Glucose		BY 4741	Y
YNB + a.a DO +2% Glucose		BY 4741 Δ Aro1	N
YNB Δ (NH ₄) ₂ SO ₄ + a.a DO + 2% Glucose		BY 4741	Y
YNB Δ (NH ₄) ₂ SO ₄ + a.a DO + 2% Glucose		BY 4741 Δ Aro1	N
YNB + a.a DO + 2% Glucose + 25 mg/L Chorismate		BY 4741 Δ Aro1	N
YNB Δ (NH ₄) ₂ SO ₄ + a.a DO + 2% Glucose + 25 mg/L Chorismate		BY 4741 Δ Aro1	N
YNB + a.a DO + 2% Glucose (BY 4741 Δ Aro1)	Y/N (#)	YNB Δ (NH ₄) ₂ SO ₄ + a.a DO + 2% Glucose (BY 4741 Δ Aro1)	Y/N (#)
30 mg/L Tyrosine + 40 mg/L Tryptophan + 50 mg/L Phenylalanine	Y	30 mg/L Tyrosine + 40 mg/L Tryptophan + 50 mg/L Phenylalanine	Y
60 mg/L Tyrosine	Y	60 mg/L Tyrosine	Y (267)
		180 mg/L Tyrosine	Y (102)
40 mg/L Tryptophan	Y	40 mg/L Tryptophan	Y (181)
		80 mg/L Tryptophan	Y (351)
100 mg/L Phenylalanine	N	100 mg/L Phenylalanine	N
		200 mg/L Phenylalanine	N
60 mg/L Tyrosine + 100 mg/L Phenylalanine	N	60 mg/L Tyrosine + 100 mg/L Phenylalanine	N
40 mg/L Tryptophan + 60 mg/L Tyrosine	Y (184)	40 mg/L Tryptophan + 60 mg/L Tyrosine	Y (313)
40 mg/L Tryptophan + 100 mg/L Phenylalanine	Y (149)	40 mg/L Tryptophan + 100 mg/L Phenylalanine	Y (94)

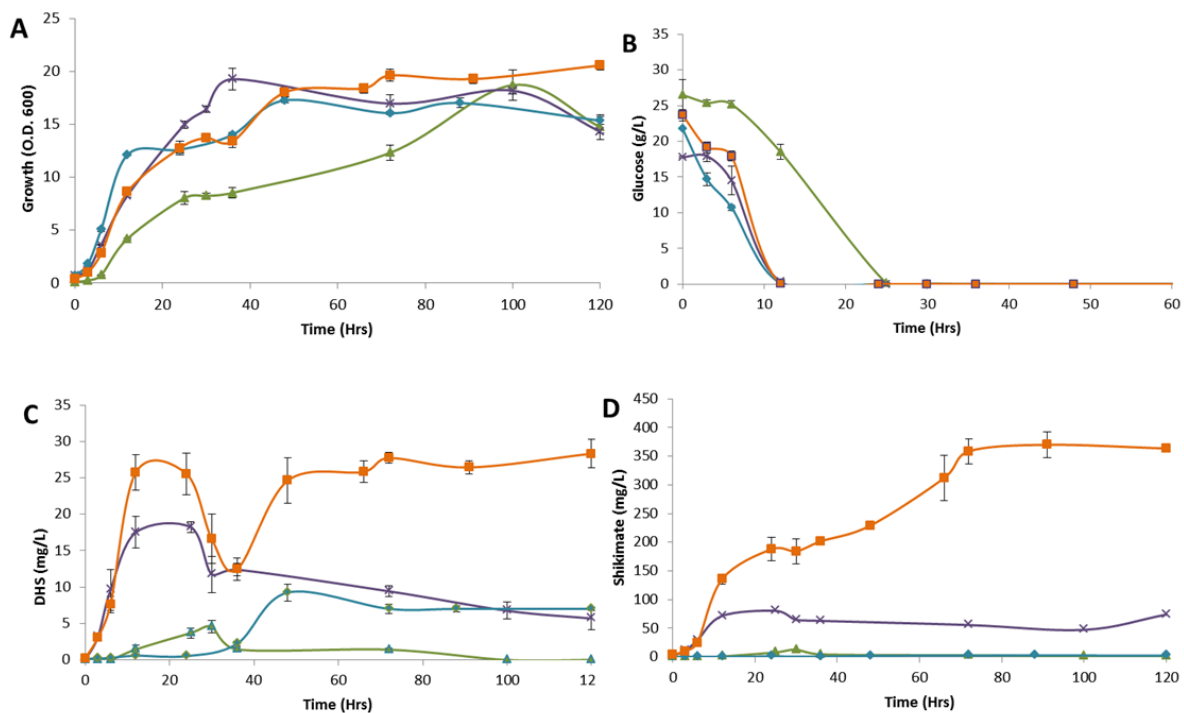


Figure 8. Comparison of growth and metabolite accumulation by strains K34pEV, K34p4BD, 13DpEV and 13Dp4BD. They are represented by (◆), (■), (▲) and (×) respectively. **A)** Growth profiles of the 4 strains as grown in 50 ml YNB+2%glucose+0.1X dropout+35mg/L tryptophan. **B)** Glucose consumption by the four strains. 13DEV consumes glucose slower than the other strains. **C)** 3-Dehydroshikimate (DHS) accumulation by the strains. **D)** Shikimate accumulation of the 4 strains. K34p4BD accumulates 369.9 ± 29.2 mg/L of shikimate as compared to 13.1 ± 1.6 by 13DpEV. All errors represent standard deviation of biological triplicates.

Chorismate was not able to rescue growth phenotype in the presence or absence of ammonium sulphate as a nitrogen source either¹¹⁶. Additional amounts of phenylalanine inhibited growth even in the presence of tyrosine. However, the growth phenotype was rescued by tryptophan, even in the presence of phenylalanine. Tryptophan and tyrosine both rescued the growth phenotype of the *Δaro1* strain, however, tryptophan was chosen as the aromatic molecule substitute as a lesser amount of it was necessary to restore growth.

The *aro1* gene locus was completely deleted from the K34 strain using homologous recombination with LoxP-flanked antibiotic cassettes¹¹². The resulting CEN.PK *aro3 aro4 aro1 ura3* strain was named K341 (Table 1). As expected, it had a poor growth phenotype on minimal or synthetic complete media. The optimum growth conditions for K341 were determined by growing it in different concentrations of amino acid and vitamin supplementation (Figure 9A). Three times the manufacturer's recommended amount of supplementation was required to achieve K34 levels of growth. Supplementing the growth media with large amounts of aromatic molecules is not economically feasible, thus K341 was evolutionarily adapted to grow on increasingly lower amount of vitamins and amino acid supplements by growing it repeatedly and for extended periods of time in minimal media with 0.5X amino-acid dropout supplement, 35 mg/L of tryptophan but no vitamins. After multiple rounds of passage, wild-type growth phenotype was observed while growing K341 (Figure 9B). This strain was used in all further experiments.

Strain K341 pEV accumulated 14.1 ± 1 mg/L of DHS without overexpressing p4BD as compared to 9.3 ± 1.2 mg/L DHS accumulated by K34 pEV (Figure 10C). It was also observed, as expected, that there was no presence of shikimate in the cell culture (Figure 10C). However, upon overexpression of Aro4^{fbr}, AroB and AroD (p4BD) in strain K341, there was about 26.6 ± 1.6 mg/L of DHS accumulated in the cell culture, comparable to its accumulation in strain K34 p4BD (no *aro1* deletion). The deletion of *aro1* led to complete abatement of shikimate production and a 2-fold increase in DHS production as compared to the wild-type 13D strain over-expressing Aro4^{fbr}, AroB and AroD (p4BD). However, the deletion also caused the strain to be non-viable on minimal media and needing aromatic molecule supplementation to grow.

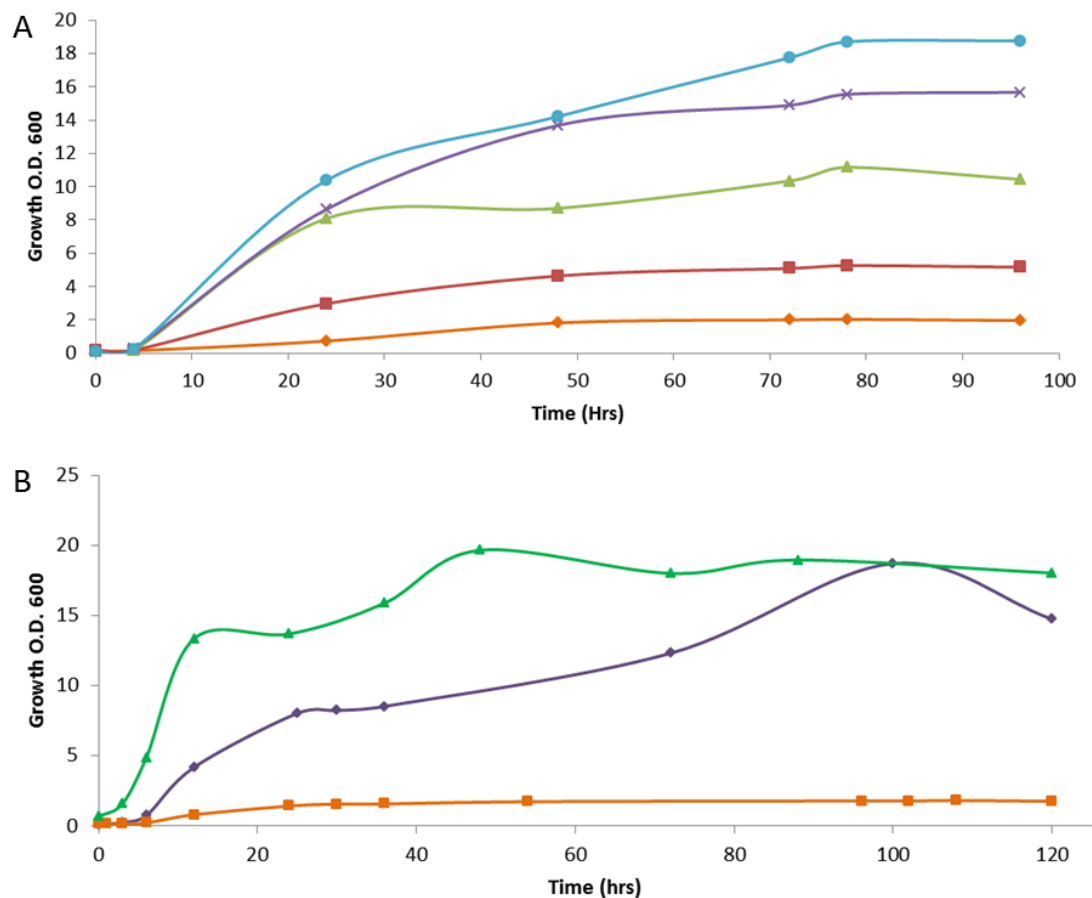


Figure 9. Effects of varying concentrations of dropout media supplementation and evolutionary adaptation on growth profiles of K341. A) Effects of varying concentrations of dropout (DO) media supplementation on growth profiles of non-viable K341pEV strains. The highest concentration of DO supplementation, 3x is represented by (●); 2x DO supplementation is represented by (x); 1x DO is represented by (▲); 0.5x DO is represented by (■) and 0.25x DO is represented by (◆). **B)** The effect of multiple rounds of evolutionary adaptation on the growth profile of K341pEV. 13DpEV (wild-type) is represented by (♦); K341pEV before adaptation is represented by (■) and K341pEV after adaptation is represented by (▲).

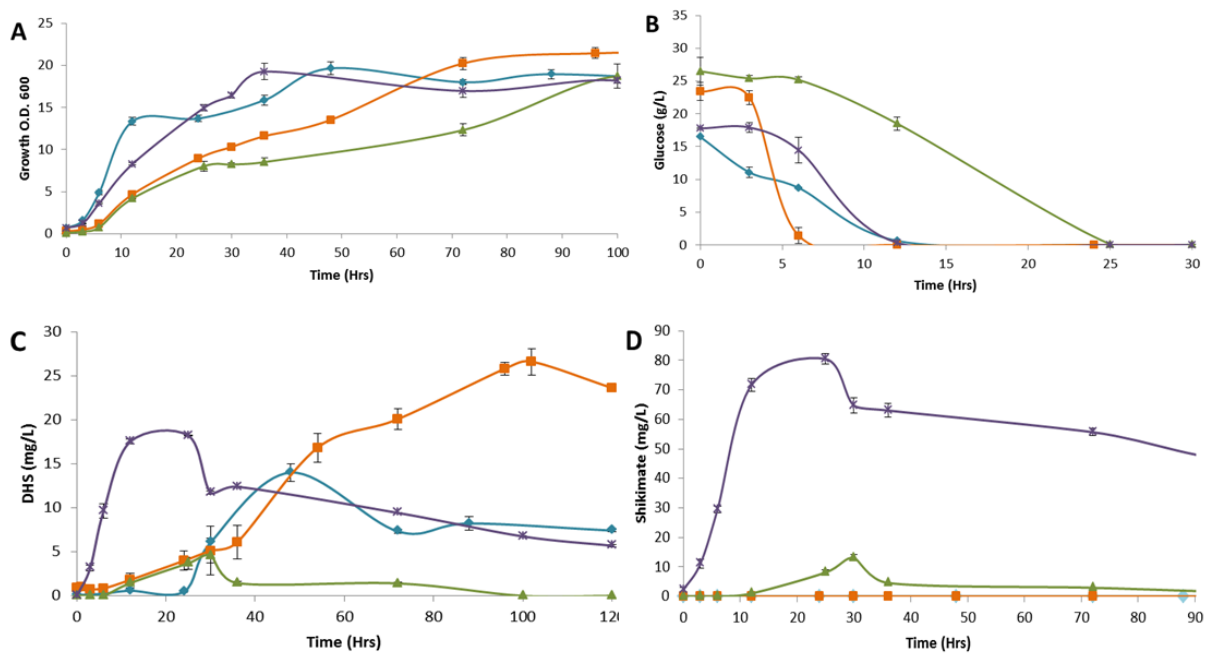


Figure 10. Comparison of growth and metabolite accumulation by strains K341pEV, K341p4BD, 13DpEV and 13Dp4BD. They are represented by (◆), (■), (▲) and (×) respectively. **A)** Growth profiles of the 4 strains as grown in 50 ml YNB+2%Glucose+0.1X Drop-Out+35mg/L tryptophan. **B)** Glucose consumption by the four strains. 13DpEV consumes glucose slower than the other strains. **C)** 3-Dehydroshikimate (DHS) accumulation by the strains. 13Dp4BD and K341p4BD accumulate more DHS than their cognate strains not expressing the p4BD plasmid. K341p4BD has a maximum accumulation of 27.1 ± 1.6 mg/L of DHS **D)** Shikimate accumulation of the 4 strains. All errors represent standard deviation of biological triplicates.

Thus, in order to have the minimal possible modification to cellular metabolism, a mutation that would minimize the conversion of DHS to shikimate by altering the active site of Aro1 was also pursued.

3.3 Effect of Mutations in Aro1 on Cellular DHS Accumulation

As deletion of *aro1* results in a large negative effect on cellular metabolism, its functionality must be diminished another way. Precise removal of the shikimate dehydrogenase domain of Aro1 would be preferable to the complete deletion of the protein. Weber *et al.*⁶⁷ attempted this by deleting the entire shikimate dehydrogenase domain. However, this strain was also auxotrophic for aromatic molecules and had to be rescued by overexpression of *E. coli* homolog AroE. As has been shown before, Aro1 does not have distinct metabolic channeling functions⁸⁵ and merely deleting the domain from the pentafunctional enzyme and replacing it with the cognate *E. coli* functional enzyme, AroE, would not have much of an effect in dampening the conversion of DHS to shikimic acid. Additionally, it has also been shown that any disruption in the tertiary and quaternary structure of Aro1 has negative effects on its function⁹⁰. Aro1 functions as a homo-dimer with the shikimate dehydrogenase domain as one of the dimerization interfaces. Thus, deletion of the shikimate dehydrogenase domain would have some adverse effects on Aro1's functionality. On the other hand, mutation of the active site of the shikimate dehydrogenase domain to decrease its catalytic activity would have the desired effect of disrupting the conversion of DHS to shikimic acid.

There are multiple highly conserved amino acid residues in the shikimate dehydrogenase active site that convert DHS to shikimate using NADPH as a cofactor. Most of these residues are in the NADPH binding domain; however there is a conserved lysine (K) residue in the DHS binding pocket that has been implicated in DHS binding stabilization. This residue was targeted and a single point mutation was made using CRISPR mediated recombination changing the positively charged lysine residue into a negatively charged glutamic acid residue with the intention of disrupting the stabilizing effect. This strain, *S. cerevisiae* CEN.PK 13D *aro3 aro4 ura3 aro1*^{K1370E} was named K34M (Table 1).

K34M showed wild-type growth and glucose consumption phenotypes in minimal media in the presence or absence of Aro4^{fbr}, AroB and AroD (p4BD) over-expression without any need for evolutionary adaptation (Figure 11A& 11B). Without the over-expression of proteins encoded by p4BD K34M pEV accumulated 8.5 ± 0.2 mg/L of DHS, comparable to DHS accumulation in strain K34 pEV and double the DHS accumulation in wild-type strain 13D pEV (Figure 11C). Over-expression of Aro4^{fbr}, AroB and AroD (p4BD) in K34M results in an accumulation of 43 ± 1.9 mg/L of DHS. This is 1.5-fold increase in the DHS accumulated by the strains K34 p4BD and K341 p4BD. Strain K34M p4BD also had a drastically reduced accumulation (≈ 20 -fold less) of shikimate, 4.8 ± 0.1 mg/L, as compared to strain 13D p4BD, 80.5 ± 1.8 mg/L (Figure 11D). K34M p4BD also had a 79-fold decrease in shikimate accumulation as compared to K34 p4BD. Thus, modulating the catalytic activity of Aro1 resulted in an increased accumulation of DHS and a decrease in shikimate production. Along with the catalytic functionality of Aro1, the abundance of Aro1 and its effect on DHS accumulation was also investigated.

3.4 Effect of Decreasing the Abundance of Aro1 on DHS Accumulation

The mutation of the shikimate dehydrogenase domain in Aro1 dramatically reduces the conversion of DHS to shikimate, increasing the intracellular pool of DHS. This resulted in more carbon being diverted from native metabolism into the heterologous pathway.

A similar effect can also be achieved by decreasing the abundance of the entire Aro1 as a whole. Decreasing Aro1's abundance will decrease the number of enzymatic domains in the cell that can convert DHS to shikimate causing a greater accumulation of DHS. This was achieved by tagging the Aro1 protein with a constitutive degradation tag that rapidly degrades the protein. Most of these tags originate from cyclin proteins that control cell cycle, hence their expression and degradation is tightly controlled to prevent cell-cycle de-regulation. Cln2 is a *S. cerevisiae* G1-cyclin that is involved in the G1 to S phase transition and is subsequently rapidly degraded. Cln2 is targeted for degradation via a proline, glutamine, serine and threonine rich tag

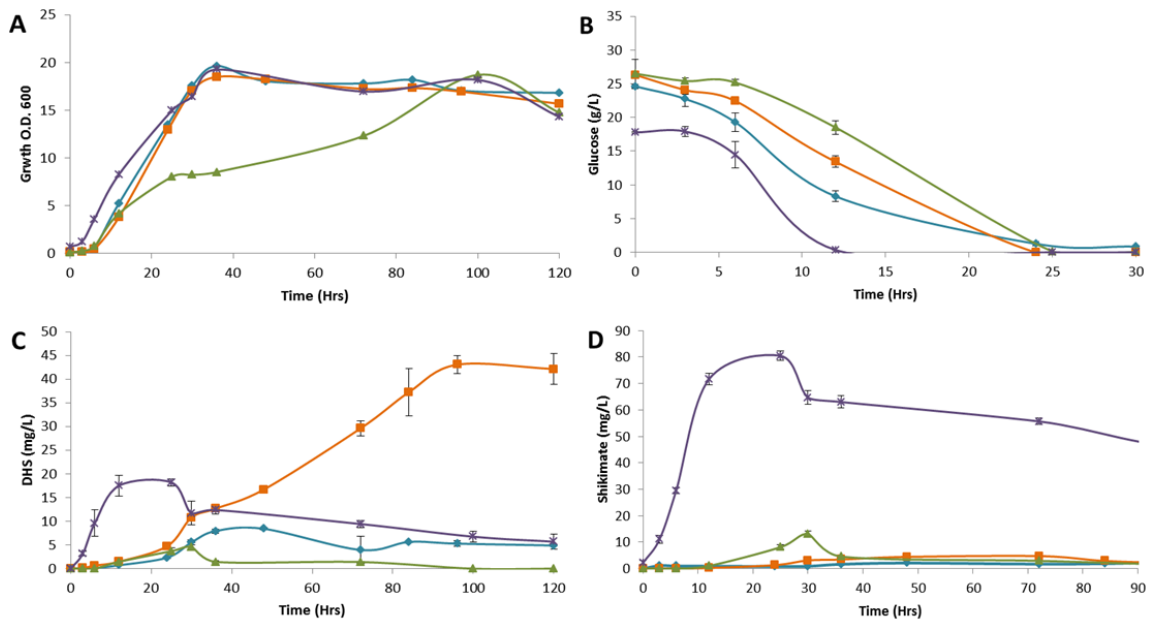


Figure 11. Comparison of growth and metabolite accumulation by strains K34MpEV, K34Mp4BD, 13DpEV and 13Dp4BD. They are represented by (◆), (■), (▲) and (×) respectively. **A)** Growth profiles of the 4 strains as grown in 50 ml YNB+2%Glucose+0.1X Dropout+35mg/L tryptophan. **B)** Glucose consumption by the four strains. 13DpEV consumes glucose slower than the other strains. **C)** 3-Dehydroshikimate (DHS) accumulation by the strains. K34Mp4BD has a maximum accumulation of 43.1 ± 1.9 mg/L of DHS. **D)** Shikimate accumulation of the 4 strains. 4.7 ± 0.1 mg/L is the maximum shikimate accumulated by K34Mp4BD. All errors represent standard deviation of biological triplicates.

sequence (PEST tag) that targets the protein for degradation by the constitutive ubiquitin pathway.

The PEST tag from Cln2 was inserted in the 3' end of Aro1 using CRISPR mediated recombination. This strain, *S. cerevisiae* CEN.PK 13D *aro3 aro4 ura3 aro1-Cln2_{PEST}*, was named K34A1Cln2 (Table 1).

Strains K34A1Cln2 pEV and K34A1Cln2 p4BD showed wild-type growth profiles in minimal media demonstrating that there was no detrimental effect on cell viability (Figure 12A& 12B). K34A1Cln2 pEV accumulated only 0.8 ± 0.1 mg/L of DHS which is 4-fold less than the amount of DHS accumulated by 13D pEV (Figure 12C). Strain K34A1Cln2 p4BD accumulated 32.3 ± 3.3 mg/L of DHS, which is greater than the amount of DHS accumulated by strains K34 p4BD and K341 p4BD and double the amount of DHS accumulated by strain 13D p4BD. Strain K34A1Cln2 pEV also accumulated 11.1 ± 0.2 mg/L of shikimate which is less than the amount of shikimate accumulated by strain 13D pEV (13.1 ± 1 mg/L), but greater than the amount accumulated by strain K34M pEV, 2.1 ± 0.1 gm/L (Figure 12D). Expression of Aro4^{fbr}, AroB and AroD (p4BD) in K34A1Cln2 increased shikimate accumulation to 94.8 ± 3.5 mg/L, which is 20-fold higher than the shikimate accumulation in strain K34M p4BD and comparable to the shikimate accumulation in 13D p4BD. However, the shikimate accumulation in strain K34A1Cln2 p4BD is 4-fold smaller than the accumulation in strain K34 p4BD demonstrating the effectiveness of degrading Aro1 in the effort to increase the accumulation of DHS by decreasing the conversion of DHS to shikimate. De-regulation of the feedback inhibition in the aromatic pathway and over-expression of the AroB and AroD enzymes coupled with the decrease in the shikimate dehydrogenase activity in Aro1 has resulted in strains that accumulate a greater amount of DHS and smaller amounts of shikimate as compared to wild-type strains without any discernable decrease in growth fitness (Figure 13). These strains would be more efficient at diverting carbon away from native aromatic molecule biosynthesis and into the heterologous CCM pathway.

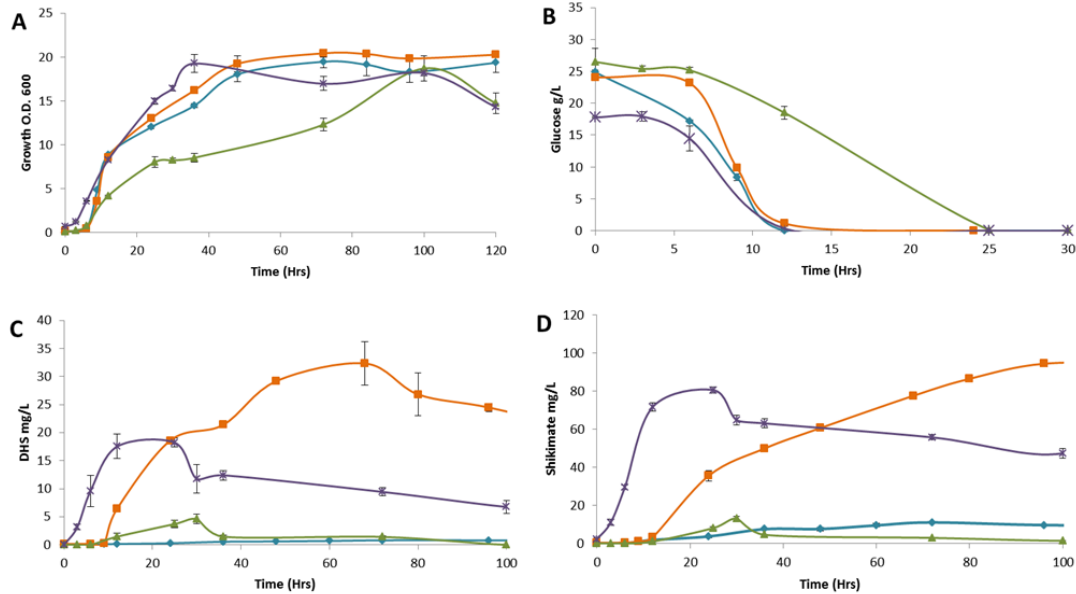


Figure 12. Comparison of growth and metabolite accumulation by strains K34Cln2MpEV, K34Cln2p4BD, 13DpEV and 13Dp4BD. They are represented by (◆), (■), (▲) and (×) respectively. **A)** Growth profiles of the 4 strains as grown in 50 ml YNB+2%Glucose+0.1X Dropout+35mg/L tryptophan. **B)** Glucose consumption by the four strains. 13DEV consumes glucose slower than the other strains. **C)** 3-Dehydroshikimate (DHS) accumulation by the strains. K34Cln2p4BD has a maximum accumulation of 32.3 ± 3.9 mg/L of DHS **D)** Shikimate accumulation of the 4 strains. K34Cln2p4BD has a markedly decreased accumulation of shikimate as compared to K34p4BD at 94.8 ± 3.5 mg/L. All errors represent standard deviation of biological triplicates.

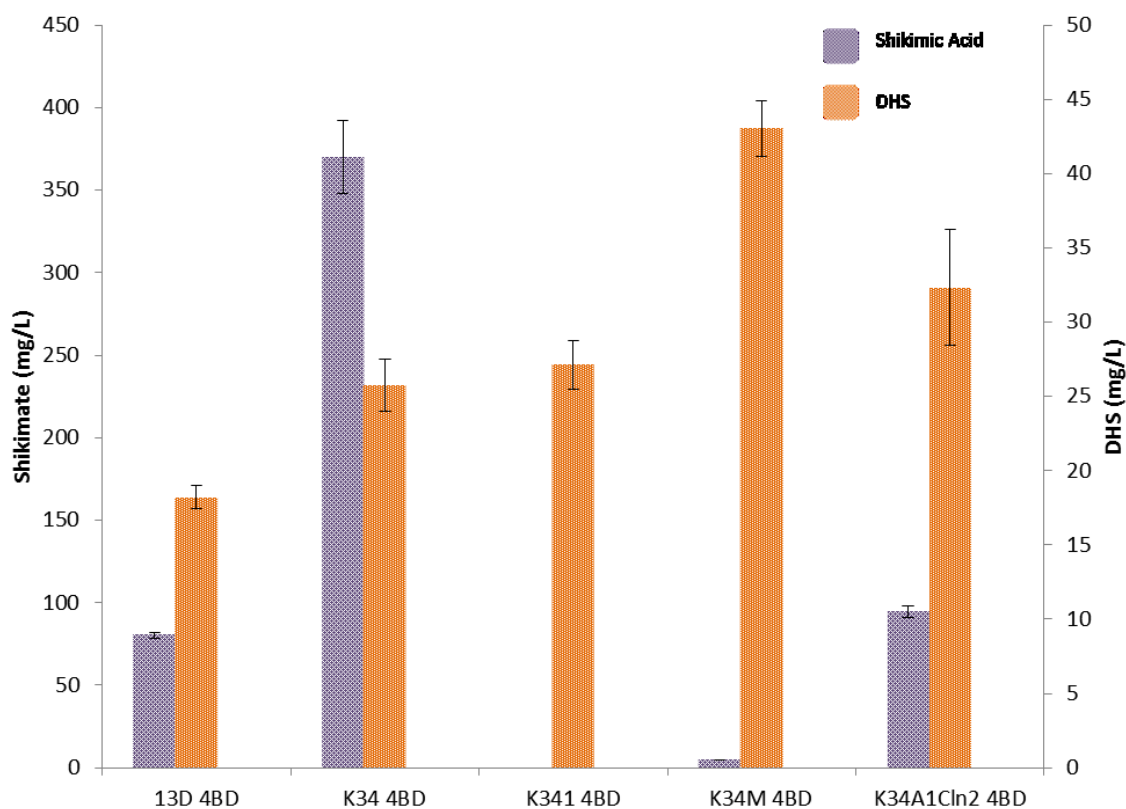


Figure 13. Comparison of the maximum accumulation of shikimate and 3-dehydroshikimate (DHS) in 13Dp4BD, K34p4BD, K341p4BD, K34Mp4BD and K34Cln2p4BD. K34p4BD has the maximum accumulation of shikimate at 369.9 ± 22.2 mg/L and K34Mp4BD has the lowest at 4.8 ± 0.1 mg/L. K34Mp4BD also accumulated the largest amount of DHS in the compared strains at 43.1 ± 1.9 mg/L. All standard deviations are based on the result of biological triplicates.

3.5 Effect of Optimizing DHS Accumulation on Carbon Flux into Heterologous CCM Pathway

Cis, cis-Muconic acid (CCM) is a heterologous compound that is produced from native aromatic molecule precursors via a heterologous enzyme pathway. 3-Dehydroshikimate (DHS) is converted into protocatechuic acid (PCA) via a DHS dehydratase, AroY, from *P. anserina*. PCA is decarboxylated to catechol by a protocatechuic acid decarboxylase (PCAD), AroZ from *K. pneumoniae*. Catechol is finally converted to CCM via an oxygen-dependent ring opening step catalyzed by a catechol-di-oxygenase (CDO), Hqd2, from *C. albicans*. The production of CCM depends on the amount of carbon diverted into the pathway from native aromatic molecule biosynthesis and the catalytic efficiency of the heterologous enzymes.

In the previous section the accumulation of DHS as a precursor was optimized by removing the native feedback inhibition on the aromatic pathway and minimizing the conversion of DHS into shikimate. In order to increase DHS accumulation, by minimizing its conversion to shikimate, the native Aro1 was deleted or modified to reduce its functionality. In this section the effects of these modifications on the production of CCM and its precursors will be explored.

Addition of the 6 gene plasmid to the wild-type 13D strain (Strain 13D p6g, Table 1) resulted in the production of PCA, catechol and CCM. After 120 hours of shake flask cultivation in minimal media with supplementation there was an accumulation of 157.5 ± 3.2 mg/L of PCA demonstrating that carbon was being channeled from native metabolism into the heterologous CCM pathway (Figure 14D). There was also 23.7 ± 0.2 mg/L of shikimate being accumulated (Figure 14C). This implies that there was still a large amount of shikimate being produced by the cells. Further down the heterologous pathway, 0.53 ± 0.05 mg/L of catechol and 1.59 ± 0.08 mg/L of CCM were accumulated, validating the functionality of the heterologous pathway (Figure 14 E& 14F). This strain also accumulated 2.66 ± 0.15 mg/L of DHS, which is considerably less than the DHS accumulated by strain 13D p4BD, which is not expressing the CCM producing pathway (Figure 14B). So, this demonstrates the functionality of the CCM pathway in channeling DHS from native metabolism and producing CCM and its heterologous precursors.

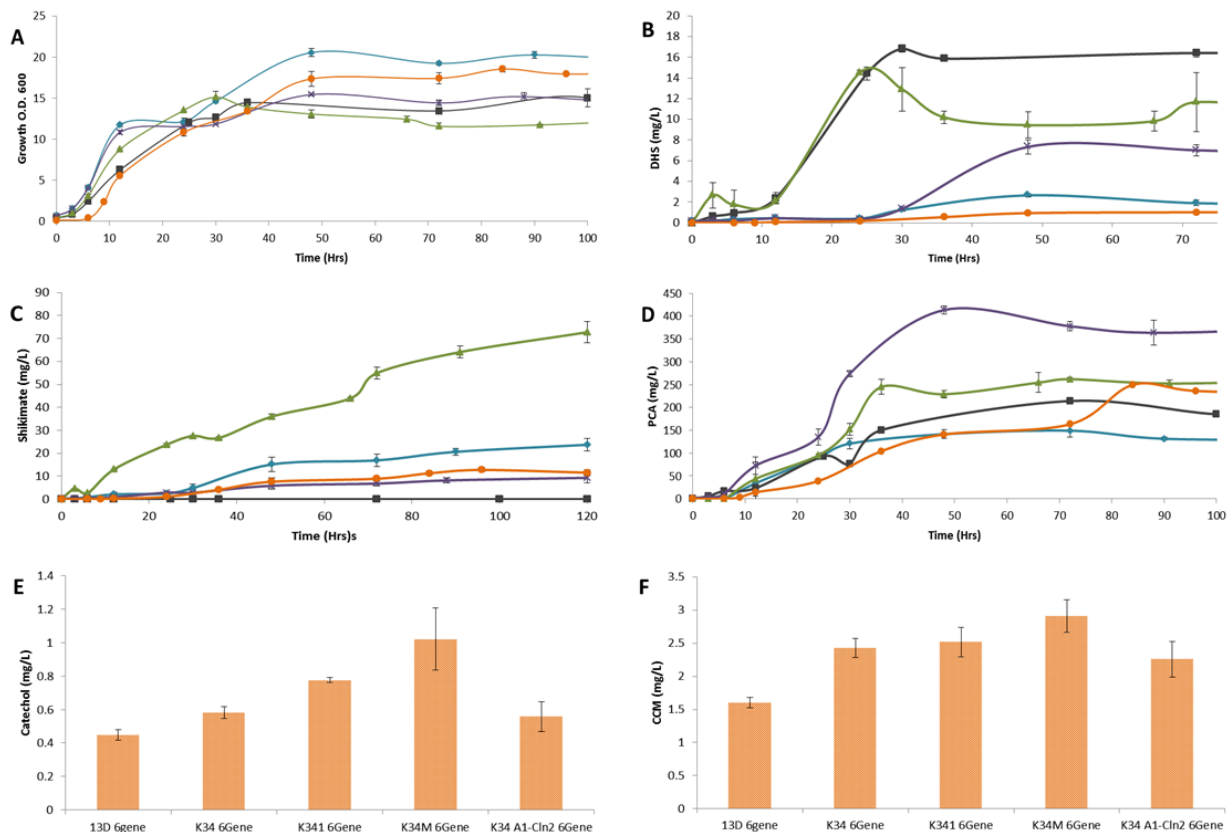


Figure 14. Comparison of growth and metabolite accumulation by strains 13Dp6g, K34p6g, K341p6g, K34Mp6g and K34A1Cln2p6g. They are represented by (◆), (▲), (■), (x) and (●) respectively. **A)** Growth profiles of the 5 strains as grown in 50 ml YNB+2%Glucose+0.1X Dropout+35mg/L tryptophan. **B)** 3-dehydroshikimate (DHS) accumulation by the strains. K341p6g and K34p6g, at 16.8 ± 0.4 mg/L and 14.5 ± 0.2 mg/L, accumulate more DHS than the other measured strains. **C)** Shikimate accumulation of the 5 strains. **D)** Accumulation of protocatechuic acid (PCA) in the strains. K34Mp6g accumulates the greatest amount of PCA at 413.2 ± 8.4 mg/L. **E)** Catechol accumulation of the 5 strains. K34Mp6g accumulated the greatest amount of catechol and 13Dp6g accumulated the least. **F)** Accumulation of *cis,cis*-muconic acid (CCM) in the strains. K34Mp6g accumulates the greatest amount of CCM and 13Dp6g accumulated the least. Errors bars represent standard deviation of biological triplicates.

As the functionality of the heterologous pathway was validated, it was introduced in the strains that were optimized for DHS accumulation.

3.5.1 Effect of Complete De-Regulation of the Chorismate Pathway on CCM Production

Strain K34 expressing Aro4^{fbr}, AroB, AroD, AroZ, AroY and Hqd2 (p6g) (Strain K34p6g, Table 1) displays a diminished growth profile as compared to K34 pEV and K34 p4BD (Figure 14A). This strain accumulated 260.2 ± 9.2 mg/L of PCA after a 120-hr fermentation (Figure 14D). As expected, this was a greater accumulation of PCA as compared to 13D p6g. Strain K34 p6g also accumulated 72.7 ± 4.7 mg/L of shikimate which is a 3-fold increase as compared to 13d p6g (Figure 14C). However, K34 p4BD accumulated 369.9 ± 22 mg/L of shikimate, so a significant amount of carbon is being channeled into the heterologous pathway in K34 p6g. Strain K34 p6g also accumulates 0.58 ± 0.04 mg/L of catechol and 2.43 ± 0.15 mg/L of CCM, a slight increase compared to the accumulation in 13D p6g (Figure 14 E& 14F). Strain K34 p6g also had a maximum DHS accumulation of 14.5 ± 0.2 mg/L which then was consumed by the cells to achieve a final accumulation of 10 ± 1 mg/L (Figure 14B). This represents more than a 50% decrease from the DHS accumulation in strain K34 p4BD demonstrating that carbon was being efficiently into the heterologous pathway but there is still room for improvement. As there is still 72.7 ± 5 mg/L of shikimate being accumulated by the over-expression of chorismate pathway and heterologous genes, the production of CCM was investigated in strains with modified Aro1 functionality.

3.5.2 Effect of Ablation of Aro1 Functionality on Carbon Flux Towards CCM Production

Similar to K34 p6g, strain K341 p6g (Table 1) also had a diminished growth profile as compared to K341 p4BD (Figure 14A). This might be due to the metabolic burden associated with the over-expression of three more enzymes for the heterologous pathway. K341 has a complete ablation of all Aro1 activity and has demonstrated a complete lack of shikimate production when the chorismate pathway enzymes were over-expressed (strain K341 p4BD). When the

heterologous CCM pathway was expressed in this strain (K341 p6g) it accumulated 214.1 ± 2 mg/L of PCA with no quantifiable shikimate production (Figure 14D). This is a slightly smaller accumulation of PCA as compared to strain K34 p6g. K341 p6g also accumulated more catechol and CCM, 0.78 ± 0.16 mg/L and 2.52 ± 0.22 mg/L respectively, as compared to K34 p6g (Figure 14 E&F). Surprisingly, strain K341 p6g had a significantly higher final accumulation of DHS, 16.8 ± 0.4 mg/L, as compared to strain K34 p6g (Figure 14B). This is still a major decrease from the amount of DHS accumulated by strain K341 p4BD; however, it highlights some carbon channeling problems into the CCM pathway.

3.5.3 Effect of Aro1^{K1370L} Mutation on Carbon Flux Towards CCM Production

The K34M strain incorporated a mutation in Aro1's shikimate dehydrogenase domain that disrupts DHS binding to the active site, effectively increasing the accumulation of DHS by preventing its conversion to shikimate. K34M p4BD accumulated large amounts of DHS and minimal amounts of shikimate. So it should be capable of channeling large amounts of DHS into the CCM pathway. Strain K34M p6g (Table 1) shows a decrease in its final biomass accumulation as compared to K34M p4BD (Figure 14A). This is consistent with the observations on strains K34 p6g and K341 p6g. Strain K34M p6g accumulated the largest amount of PCA measured in this study at 419.2 ± 8.3 mg/L (Figure 14D). This is a 2.7-fold greater accumulation of PCA as compared to strain 13D p6g, and is 1.6- and 1.9-fold greater than the amount of PCA accumulated by K34 p6g and K341 p6g respectively. Strain K34M p6g also accumulated 9.3 ± 2.3 mg/L of shikimate (Figure 14C). This is 1.4-fold less than the basal amount of shikimate accumulated by the wild-type strain not over-expressing any of the chorismate pathway enzymes (strain 13D pEV). Strain K34M p6g also accumulated small amounts of DHS at 7.3 ± 0.7 mg/L (Figure 14B). This is comparable to the basal amount of DHS accumulated by strain 13D pEV. So, most of the carbon going into the chorismate pathway was successfully diverted into the CCM pathway. Using all this carbon, strain K34M p6g accumulated 1.02 ± 0.19 mg/L of catechol and 2.91 ± 0.24 mg/L of CCM (Figure 14E & 14F). This accumulation would point to significant carbon flux problems downstream of PCA production in the CCM pathway, as addressed by Curran *et al.*⁶⁹. So, the Aro1 mutation successfully minimizes the conversion of

DHS into shikimate and further native aromatic molecules and channels more carbon towards CCM production.

3.5.4 Effect of Decreasing Aro1 Abundance on Carbon Flux Towards CCM Production

As seen earlier (Figure 12), decreasing the abundance of Aro1 had considerable effects on DHS accumulation. Strain K34A1Cln2 p4BD accumulated 32.3 ± 3.3 mg/L of DHS (double the accumulation in strain 13D p4BD) and only 11.1 ± 0.2 mg/L of shikimate (comparable to strain 13D pEV). Expression of the CCM pathway in this strain should divert most of the carbon away from the native chorismate pathway.

Expression of the CCM pathway in strain K34A1Cln2 (K34A1Cln2 p6g, Table 1) resulted in a diminished growth profile as observed before with all the CCM producing strains (Figure 14A). K34A1Cln2 p6g accumulated 249.5 ± 7.6 mg/L of PCA, which is comparable to the PCA accumulation in strain K34 p6g and 1.2- and 1.6-fold higher than the PCA accumulation in strains K341 p6g and 13D p6g, respectively (Figure 14D). Thus, even with the partial loss of the native AroB and AroD functionality, which is present in strain K34 p6g, it was able to divert similar amounts of carbon into the CCM pathway. Strain K34A1Cln2 p6g also accumulated only 11.6 ± 1.4 mg/L of shikimate in the culture (Figure 14C). This is comparable to the shikimate accumulation in strains K34M p6g and 13D pEV and 8-fold smaller than the shikimate accumulation observed in strain K34 p6g, which points to the success of the DHS accumulation optimization strategy. After 120 hours of fermentation, strain K34A1Cln2 p6g accumulated 0.56 ± 0.09 mg/ of catechol and 2.25 ± 0.27 mg/L of CCM (Figure 14E& 14F). This is comparable to the catechol and CCM accumulation in all the other strains further giving strength to the argument that there are severe carbon flux problems further down the CCM pathway.

Comparing the PCA and shikimate accumulation in the strains expressing the CCM pathway will identify the strain that was most efficient in diverting carbon from the native aromatic pathway into the heterologous CCM pathway (Figure 15). Strain K341 p6g accumulated no shikimate as expected, however as the strain cannot be grown without supplementation it has a major viability issue. Strains K34M p6g and K34A1Cln2 p6g accumulated the least amount of shikimate

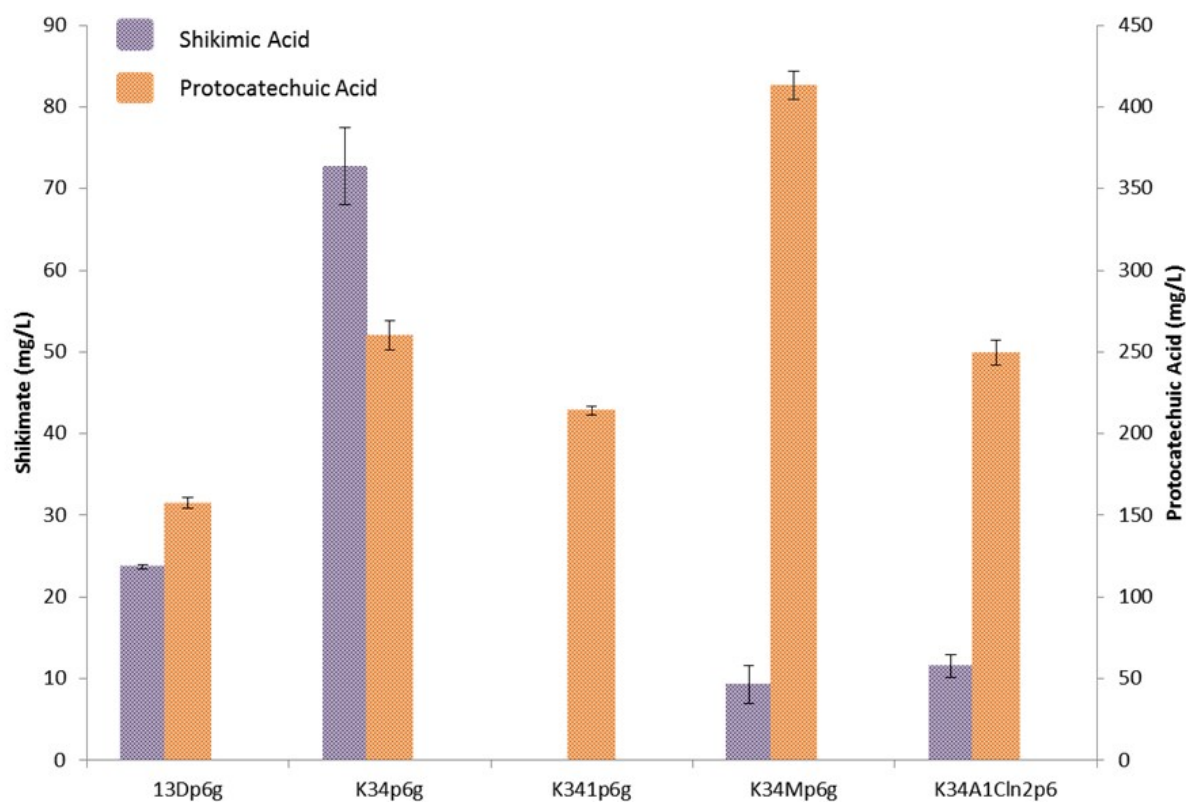


Figure 15. Comparison of the maximum accumulation of shikimate and protocatechuic acid (PCA) in CCM producing strains. K34Mp6g has the maximum accumulation of PCA at 413.2 ± 8.4 mg/L and 13Dp6g has the lowest at 157.5 ± 3.2 mg/L. K34Mp6g also accumulated the smallest amount of shikimate in the compared strains at 9.1 ± 2.3 mg/L. All standard deviations are based on the result of biological triplicates.

as compared to all the other strains and have non-affected growth profiles. Out of these strains, K34M p6g accumulated the greatest amount of PCA at 413.2 ± 8.4 mg/L. Thus, strain K34M is the best choice for a CCM producing host strain as it converted the most amount of carbon going into the chorismate pathway to PCA with the smallest accumulation of shikimate and downstream native aromatic molecules. Optimizing DHS accumulation and channeling it into the CCM pathway has resulted in large increases in the amount of PCA produced by the strains. However, not all the carbon in the form of glucose is converted to PCA. There are still large carbon sinks present in the cell.

3.6 Accumulation of Fermentation By-Products as Unwanted Carbon Sinks

As *S. cerevisiae* consumes carbon, in the form of glucose, aerobically or anaerobically it produces ethanol and acetate as by-products of fermentation, usually, to balance important redox cofactors in the cell (Figure 2). Thus, a significant portion of the carbon consumed by the cell gets converted to ethanol and acetate. As the conversion of DHS to shikimate is NADPH dependent, removing the shikimate dehydrogenase functionality and increasing the carbon flux into the chorismate pathway will likely have an effect on ethanol and acetate accumulation in the cell. Moreover, as the complete chorismate pathway consumes additional glycolytic precursors apart from the first condensation step between E4P and PEP, changing the flux through this pathway might create metabolic bottlenecks that could result in changes to ethanol and acetate production. To this effect, the ethanol and acetate accumulations in each of the strains were measured.

Without any over-expression of the chorismate pathway enzymes, the wild-type strain 13D pEV produced 2.8 ± 0.4 g/L of ethanol and had a maximum accumulation of 164.8 ± 13.3 mg/L of acetate. The deletion of the DAHP synthases (*aro3* and *aro4*) in strain K34 pEV doubled the production of ethanol at 5.6 ± 0.3 g/L (Figure 16A). However, the amount of acetate accumulated by the strain was comparable to the amount accumulated by 13D pEV (Figure 16B). Deletion of the Aro1 protein did not significantly change the ethanol production of the strain and is comparable to the ethanol production of 13D pEV. On the other hand, acetate

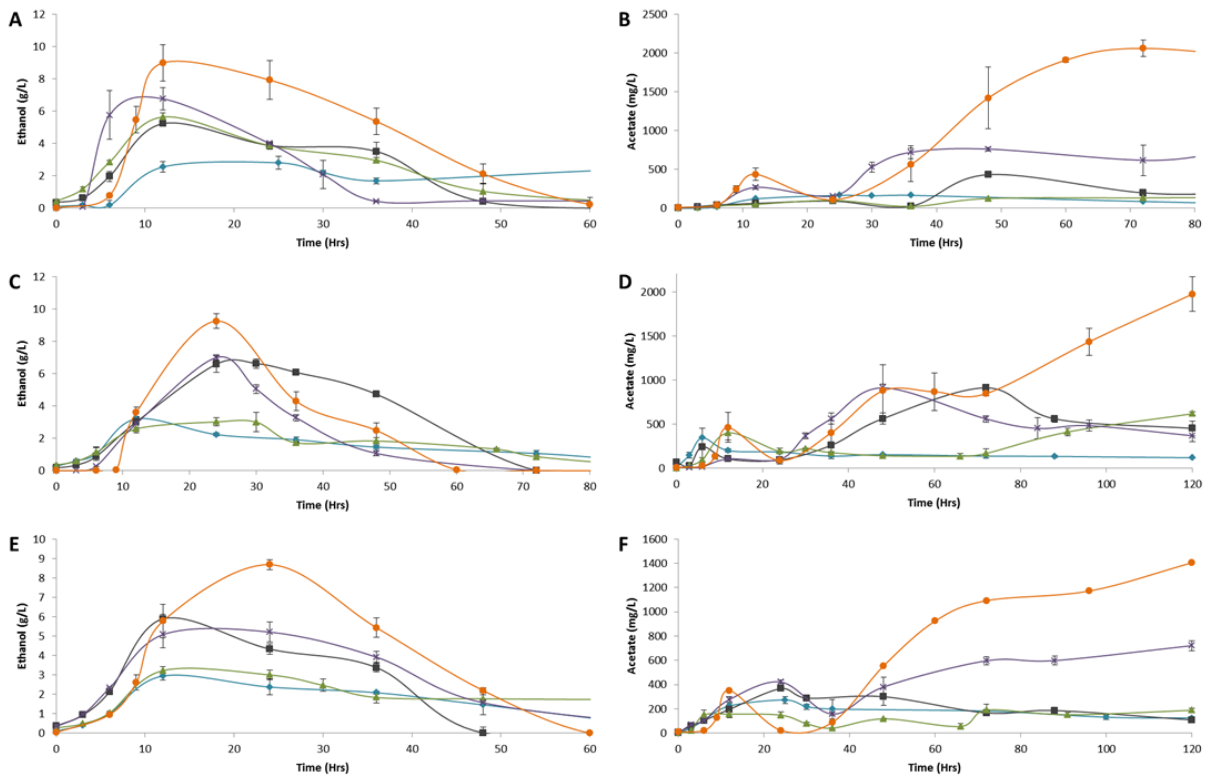


Figure 16. Comparison of ethanol and acetate production by strains 13D, K34, K341, K34M and K34A1Cln2. They are represented by (◆), (▲), (■), (×) and (●) respectively. **A)** Ethanol production in strains expressing pEV plasmid representing the basal ethanol production in these strains. **B)** Acetate production in strains expressing pEV plasmid representing the basal ethanol production in these strains. **C)** Ethanol production in strains expressing p4BD plasmid that deregulates the chorismate pathway. **D)** Acetate production in strains expressing p4BD plasmid that deregulates the chorismate pathway. **E)** Ethanol production in strains expressing p6g plasmid that deregulates the chorismate pathway and expresses the heterologous *cis*, *cis*-muconic acid producing pathway **D)** Acetate production in strains expressing the proteins encoded by the p6g plasmid that deregulate the chorismate pathway and expresses the heterologous *cis*, *cis*-muconic acid producing pathway. All errors bars represent standard deviation of biological triplicates.

accumulation in strain K341 pEV reached 431.4 ± 36.9 mg/L, which is a 2.5-fold increase as compared to acetate accumulation in strain 13D pEV. Similarly, modifying the Aro1 shikimate dehydrogenase domain and decreasing the abundance of the Aro1 drastically changed the accumulation profiles of ethanol and acetate. K34M pEV produced 6.7 ± 0.7 g/L of ethanol and 852.6 ± 45.6 mg/L of acetate, which is a 4-fold increase in acetate accumulation as compared to strains K341 pEV and K34 pEV. Similarly, K34A1Cln2 pEV also accumulated large amounts of acetate and ethanol, 2057.8 ± 153.3 mg/L and 8.9 ± 1.1 g/L respectively. This represents a 3-fold increase in ethanol production and a 12-fold increase in acetate production as compared to 13D pEV. This implies that modulation of the Aro1 node has significant effects on cellular metabolism and direction of carbon in the cell.

Expression of the Aro4^{fbr}, AroB and AroD (p4BD), which expresses a feed-back inhibition resistant Aro4 mutant, AroB and AroD, significantly affects ethanol production and acetate accumulation in the strains. Strain 13D p4BD has a maximum accumulation of 3.2 ± 0.1 g/L of ethanol (Figure 16C) and 343.5 ± 10.3 mg/L of acetate (Figure 16D) after 120 hours of fermentation. This is a modest increase in accumulation as compared to 13D pEV. Strain K34 p4BD produces similar amounts of ethanol but more acetate as compared to K34 pEV at 3 ± 0.2 g/L and 617.5 ± 20.8 mg/L respectively. Complete deletion of the Aro1 protein and over-expression of the chorismate pathway had a drastic effect on ethanol and acetate production in the culture. K341 p4BD produced 6.6 ± 0.5 g/L of ethanol and accumulated 910.5 ± 43.5 mg/L of acetate. This is a 2-fold increase in ethanol production as compared to 13D p4BD and a 3-fold increase in acetate accumulation. The same trend is also seen in strain K34M p4BD. K34M p4BD had a maximum ethanol production of 7 ± 0.2 g/L representing a 2-fold increase as compared to 13D p4BD. Similarly, K34M p4BD also accumulated 918.2 ± 33.4 mg/L of acetate representing a 3-fold increase as compared to the acetate accumulation in 13D p4BD. Changing the abundance of Aro1 and overexpressing the chorismate pathway also has similar effects on ethanol and acetate production. Strain K34A1Cln2 p4BD has a maximum production of 9.2 ± 0.4 g/L of ethanol and accumulates 1972.9 ± 194.6 mg/L of acetate. This is a 3-fold increase in ethanol production and 5.6-fold increase in acetate accumulation as compared to 13D p4BD. Thus, changing the abundance of Aro1 also has major changes on the flow of carbon through

the cell. The over-expression of the chorismate pathway enzymes only exacerbates this phenotype, hinting at a possible metabolic bottleneck or redox imbalance.

Expression of the heterologous pathway in these strains decreased the overall ethanol production and acetate accumulation as compared to simply over-expressing the chorismate pathway enzymes (Figure 16 E& 16F). The relative production and accumulation profiles of the different strains expressing the p6g plasmid are similar to those of the strains harboring the p4BD plasmid; just the total amounts produced are lower. This could be due to the lower accumulation of biomass in these strains or more carbon being pulled into the heterologous pathway and not into the cells native carbon sinks.

These observations demonstrate that the chorismate pathway is essential in yeast's central metabolism and any modulation of the Aro1 protein or over-expression of the chorismate pathway can drastically change the flow of carbon through the cell's metabolism.

3.7 Exploring the Effect of Two-step Fermentation of K341 on CCM and PCA Production

In a recent publication Horwitz *et al.* attempted to produce CCM in *S.cerevisiae* using a $\Delta aro1$ strain⁷⁷. This study drew heavily from the work Curran *et al.*⁶⁹ did to optimize CCM production in *S. cerevisiae*. Following a similar methodology, one copy of *aroF*, *aroB*, *aroD*, *aroZ* and *catA* and 6 copies of *aroY* were integrated into the *aro1*-coding region. This created a strain that was deficient in Aro1 functionality but expressed the heterologous CCM pathway. As the deletion of Aro1 functionality resulted in a strain that was deficient in aromatic amino acids and molecules, it could not grow in minimal production media. No effort was made to evolutionarily adapt the strain to accept minimal quantities of fed aromatic amino acids. Instead, the inability of the strain to create biomass in minimal media was used as a metabolic switch to control CCM production. The strain was first grown in 96-well shake plates in rich YPD media for 48 hours to accumulate biomass, and then the cells were transferred to minimal media containing 40 g/L of sucrose as a carbon source. As the cells were unable to replicate in the minimal media, all the consumed sucrose was channeled into the heterologous pathway resulting in an accumulation

of 2.7 g/L of PCA. This is highest reported accumulation of a heterologous aromatic molecule reported in literature demonstrating the success of the two-step fermentation process. There was an uncharacterized mutation or modification in the AroY protein that rendered it non-functional and unable to convert any of the accumulated PCA into catechol and subsequently muconic acid. The functionality of CatA was determined by feeding the strain with 1 g/L of catechol resulting in a quantifiable but unreported amount of muconic acid.

This two-step fermentation process was tested with the Aro1-deficient K341 strain. K341 lacks DAHP synthase functionality and the entirety of Aro1's functionality. Additionally, this strain was evolutionarily adapted to be able to grow in minimal media with small amounts of aromatic molecule supplementation. A 6-gene plasmid expressing one copy each of Aro4^{K229L}, AroB, AroD, AroY, AroZ and Hqd2 was expressed in this strain to provide carbon flux into the CCM pathway. This strain was then grown under similar conditions as the strain in Horwitz *et al.* After 48 hours in rich YPD media, the cells were transferred to 25 ml of minimal media containing 40 g/L glucose as a carbon source for 72 hours. The biomass accumulation of the cells stayed constant and started to decrease at the end of the fermentation as expected (Figure 17A). All the glucose was consumed in 24 hours. There was an accumulation of 2.7 ± 0.1 g/L of acetate and a maximum accumulation of 7.6 ± 0.6 g/L of ethanol, which was subsequently consumed by the strain (Figure 17D). Additionally, accumulation of 32.2 ± 4.7 mg/L of native precursor DHS was measured (Figure 17C). There was a large amount of carbon that was fed into the heterologous pathway resulting in an accumulation of 2.2 ± 0.2 g/L of PCA (Figure 17B). This is less than the amount of PCA accumulated by the strain in Horwitz *et al.* study. However, K341 p6g had a functional CCM pathway and was able to accumulate 0.95 ± 0.1 mg/L of catechol and 14.56 ± 0.88 mg/L of CCM (Figure 17C). K341 p6g did not accumulate as much PCA as the strain created by Horwitz *et al.*, however it was cultured under different carbon sources and culture conditions which may have contributed to the difference in accumulation.

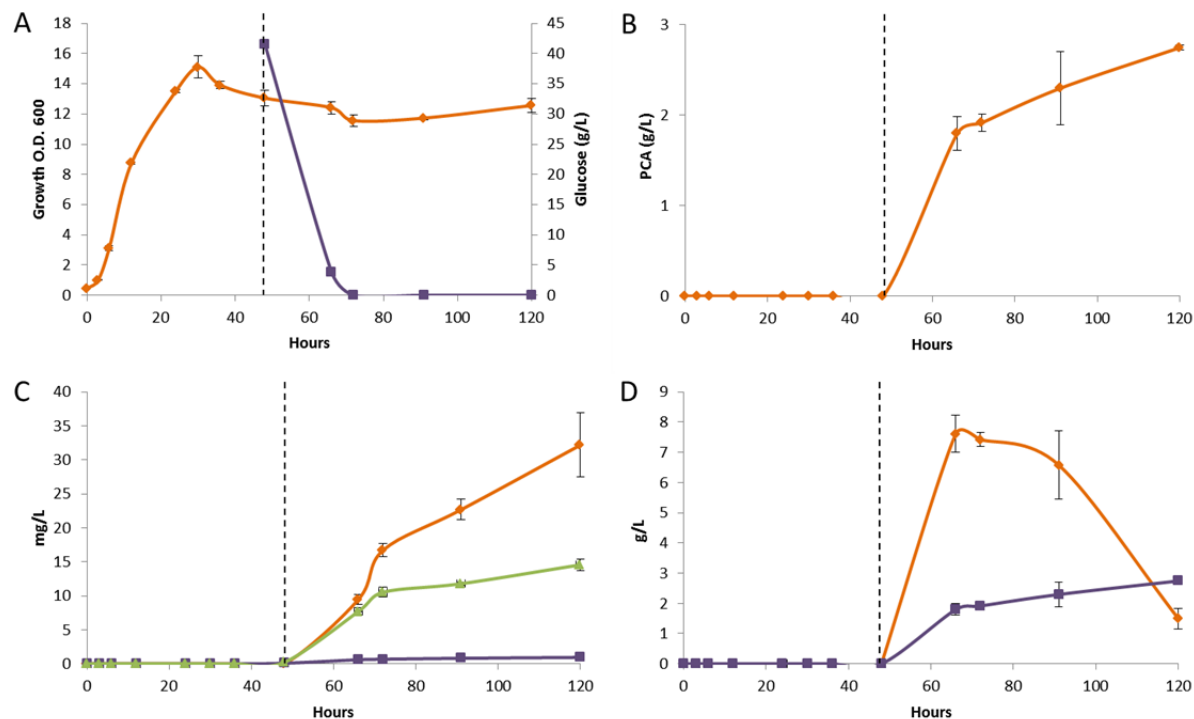


Figure 17. Comparison of growth and metabolite accumulation by K341p6g in a two-step fermentation process. The strain was grown in 25ml YPD for 48 hours and the cell pellet was collected and washed and then suspended in 25ml of YNB + 4% Glucose. The dotted line represents the time at which the growth conditions of the culture was switched **A)** Growth profile (◆) and glucose consumption (■) of K341p6g. After the cells were suspended in minimal growth media, all the glucose was rapidly consumed without any increase in biomass. **B)** Accumulation of Protocatechuic acid (PCA). Upon culturing in the minimal growth media there was a rapid production and accumulation of PCA **C)** Accumulation of 3-dehydroshikimate (DHS), Catechol and *cis,cis*-muconic acid (CCM) as represented by (◆), (■) and (▲) respectively. **D)** Accumulation of ethanol (◆) and acetate (■) in the culture. There was a maximum production of 7.60 ± 0.61 g/L of ethanol and 2.74 ± 0.03 g/L of acetate. Errors bars represent standard deviation of biological triplicates.

The two-step fermentation method has been demonstrated as an efficient and practical method of controlling the production of heterologous products in this system. However, there is still a significant metabolic block in the lower parts of the CCM pathway. This is evidenced by the large accumulation of PCA in most of the CCM producing strains contrasted by the relatively poor accumulation of catechol and CCM.

3.8 Effect of Oxygenation on PCA, Catechol and CCM Production

The relatively low accumulations of CCM and catechol were addressed and ameliorated in the study published by Curran *et al.*⁶⁹. The poor flux through the AroY enzyme that catalyzed the conversion of PCA to catechol was identified as the major problem and expressing more copies of the gene demonstrated an increase the titer of CCM to an impressive 141 mg/L. However, increasing the number of copies of a gene that are expressed, however successful, can have a limited effect on ameliorating a metabolic blockage as demonstrated by the accumulation of ≈ 300 mg/L of PCA in the high CCM producing strain. Thus there is still a significant bottleneck present in this system.

One cause of the severe restriction of the CCM pathway after PCA could be due to the oxygenation conditions of the culture. It has been previously demonstrated that the PCAD, AroY, is oxygen inhibited in its native functionality⁶⁷. This is contrasted to the functionality of the CDO, Hqd2, which performs an oxygen-dependent ring opening step. Thus, it would seem that the last two steps of the CCM pathway have opposing oxygenation requirements. The conversion of PCA to catechol would have to be performed anaerobically and the conversion of catechol to CCM would have to be in aerobic conditions. Weber *et al.*⁶⁷, had identified a previously published but uncharacterized isoform of AroY with the accession number AB479384.1 that was reported to not be oxygen-inhibited. This protein was able to convert 80% of the supplemented PCA to catechol. However, AB479384.1 was reclassified in 2013 to AB479384.2 and the amino acid sequence of this protein is identical to all the known PCAD genes from *K. pneumoniae* and homologous to the protein sequences used by Curran *et al.* and

in this study. As a large accumulation of PCA was demonstrated by both the latter studies with minimal catechol production, it is safe to assume that the PCAD, AroY, is still oxygen inhibited.

To investigate this problem, it was decided to culture a CCM producing strain in a two-step fermentation with differing oxygen concentrations. Wild-type 13D *S. cerevisiae* was transformed with a plasmid, pDAC, which expresses a single copy of AroZ, AroY and Hqd2. This strain was then grown aerobically for 36 hours to accumulate biomass. Then 1g/L of glucose was added to the culture media, nitrogen gas was used to fill the headspace and the flasks were capped to promote anaerobic growth. After 48 hours of fermentation the caps were removed and the cultures were allowed to grow aerobically. Their growth profiles and metabolite accumulation was compared to strains that were treated equally but were left uncapped to promote aerobic growth throughout the process. The uncapped cells accumulated more biomass than the capped cells during the period of capping, however, once the caps were removed the capped strains rapidly began to accumulate biomass and close the gap between the strains (Figure 18A). The capped strains also accumulated ethanol at a slower rate than the uncapped strain. (Figure 18A) The accumulation of shikimate was similar between the two strains (Figure 18 B). The uncapped and capped strains both accumulated PCA at low concentrations, 2.8 ± 0.4 mg/L and 2.2 ± 0.1 mg/L respectively, before the capping. At 96 hours of fermentation after the strains were capped, the PCA accumulation decreased to 0.9 ± 0.07 mg/L in the capped strains as compared to an accumulation of 2.2 ± 0.1 mg/L in the uncapped strains (Figure 18C). This implies that the lack of oxygen in the culture media promoted the consumption of PCA. After the cultures were uncapped the PCA accumulation increased to 1.6 ± 0.1 mg/L. The opposite effect is seen in the accumulation of catechol between the strains. After 36 hours of fermentation, both the uncapped and capped strains had accumulated similar amounts of catechol, at 0.65 ± 0.05 mg/L and 0.58 ± 0.04 mg/L respectively. After 48 hours of oxygen limited growth, the capped strain had accumulated 1.06 ± 0.04 mg/L of catechol and the uncapped strain had accumulated 0.61 ± 0.06 mg/L of catechol. However, after being returned to aerobic growth the uncapped strain decreased its accumulation of catechol to 0.69 ± 0.14 mg/L, presumably converting it to CCM (Figure 18D). The CCM accumulation was also affected by oxygen conditions of the media.

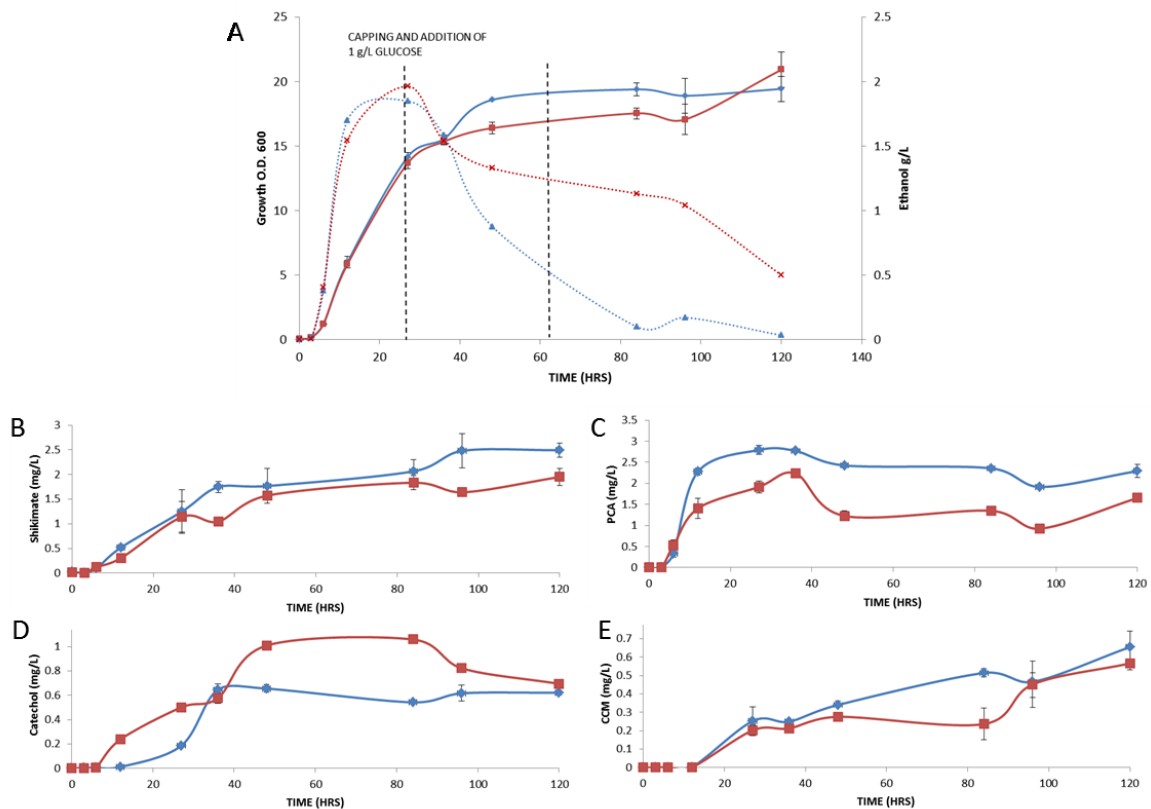


Figure 18. Comparison of growth and metabolite accumulation by 13DpDAC in an aerobic and anaerobic fermentation process. The strains that were grown aerobically are represented by (▲) and the strains that were grown aerobically for 48 hours are represented by (■). **A)** Growth profiles and ethanol production (secondary axis) of the strains. The ethanol production is represented by the dashed lines. **B)** Shikimate accumulation compared between the two growth conditions. **C)** Protocatechuic acid accumulation between the two strains with different growth conditions. **D)** Catechol accumulation between the two strains with different growth conditions. **E)** *cis,cis*-muconic acid accumulation between the two strains with different growth conditions. All errors represent standard deviation of biological triplicates.

At 36 hours of aerobic growth both the capped and uncapped strains had accumulated similar amounts of CCM, at 0.21 ± 0.03 mg/L and 0.24 ± 0.01 mg/L respectively. During the 48-hour oxygen-limited fermentation period the accumulation of CCM in the capped strain remained constant while the CCM accumulation in the uncapped strain increased to 0.514 ± 0.02 mg/L. Once the strains were allowed to grow aerobically again, the accumulation of CCM in the capped strain increased to 0.56 ± 0.12 mg/L at 120 hours, comparable to the final accumulation of 0.65 ± 0.08 mg/L in the uncapped strain (Figure 18E).

Thus, there are demonstrable effects of oxygen on the flux through the CCM heterologous pathway that need more investigation.

4. DISCUSSION

The production of adipic acid in *S. cerevisiae* would be economically, environmentally and sustainably beneficial. However, in order to have a large enough biological production system, the yields of adipic acid must be increased.

The yields of adipic acid are directly proportional to the yields of its precursor *cis,cis*-muconic acid. The production of CCM is dependent on four factors: removal of feed-back inhibition in the chorismate pathway; increasing the flux through the AroB and AroD bottleneck; the amount of DHS being converted into native aromatic molecules; and the flux through the CCM heterologous pathway.

Curran *et al.*⁶⁹ optimized the heterologous pathway to increase the flux through the rate-limiting step, the conversion of PCA to catechol, resulting in a 90-fold increase in CCM yield. The amount of carbon entering the chorismate pathway was also increased by balancing the levels of precursors E4P and PEP and removing the feedback inhibition in the chorismate pathway. Increasing the flux through the AroB and AroD node was achieved by Weber *et al.*⁶⁷ by over-expressing the *E. coli* cognate enzymes. However, modulating the loss of DHS into native metabolism has not been sufficiently addressed.

Removing the feedback inhibition in the chorismate pathway and over-expressing AroB and AroD resulted in a strain with sufficiently high carbon accumulation in the chorismate pathway to try and channel it to a heterologous pathway. The K34 p4BD strain accumulated ≈ 360 mg/L of shikimate, which represents about 2% of the carbon fed to the cells. Using K34 as a base strain three different channeling strategies were explored. The *aro1* deletion completely removed all shikimate production from the cell. However, this strategy had two negative consequences. Firstly, the strain is non-viable in minimal production media and had to be supplemented with aromatic molecules, which can get expensive in large scale fermentations. Secondly, removing Aro1 functionality also removes the native AroB and AroD functionality, which decreases the flux going through the chorismate pathway and into the heterologous pathway. This decrease in carbon flux could be the reason why strain K341 p6g did not accumulate as much PCA as K34 p6g, even with no shikimate production. Additionally, there was a large amount of DHS accumulated by strain K341 p6g as compared to the DHS accumulation in K34 p4BD or 13D p6g which points to inefficient carbon channeling. This large DHS accumulation was not seen in any of the other CCM producing strains and could be strain specific. It could point to some unknown regulation of the chorismate pathway or poor carbon utilization by the CCM pathway.

The mutation of the Aro1 shikimate dehydrogenase domain has more desirable effects on PCA accumulation. The mutation dramatically disrupted the conversion of DHS to shikimate. Strain K34M p4BD accumulated double the amount of DHS as strain K341 p4BD and almost no shikimate. In strain K34M p6g this channeling strategy was successful in diverting carbon flux from the native pathway. In 120 hours of fermentation, K34M p6g accumulated only ≈ 9 mg/L of shikimate while it accumulated ≈ 413 mg/L of PCA. This represents a 9-fold decrease in shikimate accumulation as compared to strain K34 p6g. It also represents a 72% increase in PCA accumulation as compared to K34 p6g and a 163% increase as compared to 13D p6g.

The third and final optimization strategy involved decreasing the abundance of Aro1 in order to decrease the conversion of DHS to shikimate. Although, strain K34A1Cln2 p4BD was successful in reducing the amount of shikimate accumulation as compared to K34 p4BD, the amount of

PCA accumulated by strain K34A1Cln2 p6g was similar to the amount accumulated by K34 p6g. This tells us that although the DHS accumulation optimization strategy worked, there was a decrease in carbon flux into the heterologous pathway. This is similar to K341 p6g and has the same root cause. Decreasing the abundance of Aro1 also decreases the native functionality of AroB and AroD in the strain. This led to a decrease in the amount of DHS that was produced. Thus, we can conclude that the mutation in the shikimate dehydrogenase domain of Aro1 is the most effective way to reduce the amount of carbon going into the native aromatic pathway and channel it into the CCM pathway.

The two-step fermentation with different carbon sources as demonstrated by Horwitz *et al.*⁹¹ is a practical way to use the aromatic molecule auxotrophy created by the deletion of *aro1* to our advantage. However, this method first grows the cells in rich media for 48 hours and subsequently pellets and washes the cells to remove all traces of rich media and finally suspends them in minimal production media with high amounts of carbon. These manipulations are possible in small bench-scale experiments but would be impractical and prohibitively expensive in large-scale fermentations. Additionally, there were other concerns with this strategy using strain K341. The strain used by Horwitz *et al.* accumulated 2.7 g/L of PCA while K341 p6g only accumulated 2.2 g/L. This could be explained by a number of reasons. Firstly, the Horwitz *et al.* strain was fermented in 4% sucrose while K341 p6g was fermented in 4% glucose as a carbon source. This changes the way carbon enters the glycolytic cycle in yeast. As sucrose is broken down to glucose and fructose, which are subsequently phosphorylated once they enter the cell, there is an abundance of glucose-6-phosphate and fructose-6-phosphate in the cell. Both these molecules are consumed in the glycolytic pathway; however, glucose-6-phosphate is also consumed by the pentose phosphate pathway that ultimately produces E4P. It is possible that feeding the cells both fructose and glucose channels more carbon into the pentose phosphate pathway ultimately producing more E4P. This would balance the amount of PEP and E4P produced in the cells, which was a rate-limiting step for the chorismate pathway identified by Curran *et al.*⁶⁹. Additionally, strain K341 underwent evolutionary adaptation to grow on the least amount of aromatic molecule supplementation. This adaptation could have enabled the cells to natively channel the fed carbon into aromatic molecules through

uncharacterized pathways. This would decrease the amount of carbon being shunted into the heterologous pathway leading to a comparatively lower accumulation of PCA. Therefore, evolutionarily adapting the strain, although necessary for viable growth, could have inadvertently resulted in lower yields of heterologous aromatic molecules. Though, the adaptation to much lower amounts of aromatic molecule supplementation opens the question as to what functional changes the evolutionary adaptation caused in the cells. RNAseq and metabolomics studies would have to be conducted on K341 cells to determine the exact biochemical nature of the adaptation to pinpoint the mechanism of aromatic molecule production in the Aro1 deficient strain.

The low titer of the actual desired molecule, CCM, also has to be examined. Even though there was a significant accumulation of PCA in the cells, there was very little catechol and CCM produced (Table 4). This could be because the flux through the AroY protein was really poor. However, Curran *et al.* also used one copy of the PCAD and CDO in their first strain and accumulated 15 mg/L of CCM. This would point to some unknown error in the AroY or Hqd2 protein used in this study. However, as all the constructs were sequence verified for accuracy there has to be another problem. Another obvious problem could be the oxygen-inhibition of PCAD. But, as Curran *et al.* also fermented their strain in aerobic conditions, it does not offer a satisfactory explanation. The difference in the background strains used in the two studies could be a reason for the low accumulation of catechol and CCM. Curran *et al.* used BY4741 as their background strain, while Horwitz *et al.*, Weber *et al.* and this study used CEN.PK. BY4741 and CEN.PK are not isogenic and have many uncharacterized nucleotide differences. CEN.PK has a 4.5% difference in coding regions as compared to S288C, the parent strain of BY4741¹¹⁷. These could have an uncharacterized effect on the production of aromatic molecules. However, as the differences in the strains are uncharacterized there are no definitive reasons.

The oxygenation requirements of the heterologous pathway were also examined in this study. This was done with a wild-type strain expressing the pDAC plasmid and not the high producing K34M p6g strain. As described earlier, the absence of oxygen in the anaerobic cultures led to a decrease in the accumulation of PCA and an increase in the accumulation of catechol. The

accumulation of CCM remained constant throughout the anaerobic phase. This is consistent with the oxygen inhibition of AroY and the oxygen requirement for Hqd2 functionality. Once

Table 4. Titrers and yields of metabolites in *cis,cis* muconic acid producing strains.

Strain	3-Dehydroshikimic acid		Shikimic acid		Protocatechuic Acid		Catechol		<i>cis,cis</i> Muconic Acid	
	Titer (mg/L)	Yield (mg/g glucose)	Titer (mg/L)	Yield (mg/g glucose)	Titer (mg/L)	Yield (mg/g glucose)	Titer (mg/L)	Yield (mg/g glucose)	Titer (mg/L)	Yield (mg/g glucose)
13D	2.66 ± 0.14	0.13 ± 0.01	23.71 ± 0.23	1.19 ± 0.01	213.53 ± 2.77	10.68 ± 0.14	0.45 ± 0.033	0.022 ± 0.002	1.60 ± 0.08	0.080 ± 0.004
K34	14.54 ± 0.23	0.73 ± 0.01	72.74 ± 4.69	3.64 ± 0.23	260.21 ± 9.18	13.01 ± 0.46	0.58 ± 0.037	0.029 ± 0.002	2.43 ± 0.15	0.121 ± 0.007
K341	16.83 ± 0.36	0.84 ± 0.02	0 ± 0	0 ± 0	214.06 ± 2.41	10.70 ± 0.12	0.78 ± 0.015	0.039 ± 0.001	2.52 ± 0.22	0.126 ± 0.011
K34M	7.35 ± 0.68	0.37 ± 0.03	9.31 ± 2.30	0.47 ± 0.12	413.19 ± 31.8	20.66 ± 1.59	1.02 ± 0.185	0.051 ± 0.009	2.91 ± 0.24	0.145 ± 0.012
K34 A1- Cln2	1.02 ± 0.08	0.05 ± 0.00	11.56 ± 1.35	0.58 ± 0.07	249.52 ± 7.58	12.48 ± 0.38	0.56 ± 0.090	0.028 ± 0.004	2.26 ± 0.27	0.113 ± 0.013

the cultures were grown aerobically again, the accumulation of catechol decreased and the accumulation of CCM increased. This tells us that any CCM producing strain needs to be fermented first in anaerobic conditions to promote the conversion of PCA to catechol, and subsequently in aerobic conditions to convert all the accumulated catechol to CCM. Otherwise, AroY could be engineered to be resistant to oxygen inhibition using directed or random mutagenesis techniques which would allow a simpler fermentation process.

In addition to precursor flux and oxygenation requirements the loss of carbon into native carbon sinks such as ethanol and acetate was also examined in this study. It was observed that any modulation to Aro1 drastically increases ethanol and acetate production in the cell. This can be explained by accumulation of phosphoenolpyruvate (PEP) because of the chorismate pathway. The accumulation of PEP as a result of erythrose-4-phosphate (E4P) being limited by the stoichiometric imbalance between the glycolytic pathway and the pentose phosphate pathway has been reported earlier^{9,69}. So forcing large amounts of carbon into the chorismate pathway without balancing the stoichiometric levels of E4P and PEP, results in an accumulation of PEP, which is subsequently converted into ethanol and acetate. Additionally, two molecules of PEP are used in the shikimate pathway; one to make DAHP and the other to make 5-enolpyruvyl-shikimate-3-phosphate (5-ESP). Removing or drastically reducing the 5-ESP production by disrupting the functionality or abundance of the shikimate dehydrogenase functionality leads to half the PEP original being used in the pathway to accumulate, which in turn would be converted to ethanol and acetate. Surprisingly, decreasing the abundance of Aro1 has a much more pronounced effect on acetate and ethanol production as compared to mutating *aro1* or deletion of the entire gene. However, it is observed that even though large amounts of ethanol are produced in the cell, it is all subsequently consumed during the stationary phase of the fermentation. On the other hand, acetate is mostly produced in the stationary phase and then accumulates in the cell. Thus, to increase the amount of CCM produced the amount of acetate accumulated must be reduced. This can be done by reducing the conversion of PEP to pyruvate, which would limit the production of acetate. The enzyme that converts PEP to pyruvate, Cdc19, is an essential enzyme so it cannot be removed entirely from the cell. However, mutations of that enzyme have been made that decrease its

functionality. The Cdc19 T21E mutant has been characterized to mimic the phosphorylated state of Cdc19 and reduce its functionality, causing an accumulation of PEP¹¹⁸. This modification would decrease the amount of acetate and ethanol produced limiting the siphoning of carbon towards undesired native yeast metabolism.

Putting it all together, in this study three important observations were made about the production process of CCM, which if addressed, could lead to strains that could be used for industrial production. Firstly, mutating the shikimate dehydrogenase domain of Aro1 causes more carbon to be diverted into the heterologous pathway by preventing the conversion of DHS to shikimate. Secondly, modulating the Aro1 node has a drastic effect on carbon flow throughout the cell as a large production and accumulation of acetate and ethanol are observed. And finally, there are opposing oxygen requirements in the CCM producing pathway which could be one of the causes of a poorly functioning PCAD enzyme.

Thus, to create a strain that produces a large amount of CCM, I would propose the following modifications. Over-expressing the transketolase, Tkl1, would balance the amounts of PEP and E4P in the cell. Deleting the native DAHP synthases and expressing the feedback inhibition resistant Aro4^{K229L} mutant that has been previously characterized should remove the feedback inhibition of the chorismate pathway. The *E. coli* AroB, and AroD should also be over-expressed to complement the native Aro1 functionality. This would, essentially, open the floodgates for the chorismate pathway, forcing a large amount of carbon into it. Next, the shikimate dehydrogenase domain should be mutated to create Aro1^{K1370E}, which would minimize the conversion of DHS to shikimate, leading to an increase in DHS accumulation. The heterologous pathway as published by Curran *et al.*⁶⁹, composing of 2-3 copies of *aroZ*, 6-7 copies of *aroY* and 2-3 copies of *hqd2*, should be added to this strain. Subsequently, this strain should be cultured with large amounts of a carbon source in a two-step process starting with a period of anaerobic growth followed by aerobic growth to accumulate large titers of CCM.

5. CONCLUSION

This study revealed multiple ways to improve the yield of heterologously produced CCM in *S. cerevisiae*. The Aro1 node of the chorismate pathway was successfully modulated to change how the carbon flows through the cell. Carbon was successfully diverted from native aromatic molecule synthesis into the heterologous pathway. Additionally, different fermentation processes were explored with the aim of increasing CCM titers. Two-step fermentations with anaerobic followed by aerobic cultivation was found to reduce the accumulation of intermediated in the CCM pathway and accumulate more CCM. And finally, effects of modulating Aro1 functionality on ethanol and acetate production in the cell were characterized. This can all be amalgamated into one strain that will be used to produce CCM on an industrial scale so we can wean ourselves off our dependency on non-renewable and polluting sources of raw production materials.

BIBLIOGRAPHY:

1. McKetta, J. J. *Encyclopedia of Chemical Processing and Design: Volume 2 - Additives to Alpha*. (Taylor & Francis, 1977).
2. Polen, T., Spelberg, M. & Bott, M. Toward biotechnological production of adipic acid and precursors from biorenewables. *J. Biotechnol.* (2013).
3. Burgard, A. P., Pharkya, P. & Osterhout, R. E. Microorganisms for the production of adipic acid and other compounds. (2011). at <<http://www.google.com/patents/US8062871>>
4. Wu, L., De Wildeman, S. M. A., Van Den Berg, M. A. & Trefzer, A. C. Adipate (ester or thioester) synthesis. (2011). at <<http://www.google.com/patents/US20110091944>>
5. Vyver, S. Van De & Román-Leshkov, Y. Emerging catalytic processes for the production of adipic acid. *Catal. Sci. Technol.* **3**, 1465 (2013).

6. Opec. *World Oil Outlook 2012*. (2012).
7. Barchart.com. End of day Commodity Futures Price Quotes for Crude Oil WTI (NYMEX). (2015). at <<http://www.nasdaq.com/markets/crude-oil.aspx?timeframe=5y>>
8. OrbiChem, T. *CHEMICAL MARKET INSIGHT AND FORESIGHT - Adipic Acid*. at <[http://www.orbichem.com/userfiles/CNF Samples/ada_13_11.pdf](http://www.orbichem.com/userfiles/CNF_Samples/ada_13_11.pdf)>
9. Niu, W., Draths, K. M. & Frost, J. W. Benzene-free synthesis of adipic acid. *Biotechnol. Prog.* **18**, 201–11 (2002).
10. University of York. Nitric Acid. *The Essential Chemical Industry Online 3* at <<http://www.essentialchemicalindustry.org/chemicals/nitric-acid.html>>
11. Cavani, F. & Alini, S. in *Sustainable Industrial Chemistry* 367–425 (Wiley-VCH Verlag GmbH & Co. KGaA, 2009). doi:10.1002/9783527629114.ch7
12. Alini, S., Basile, F., Blasioli, S., Rinaldi, C. & Vaccari, A. Development of new catalysts for N₂O-decomposition from adipic acid plant. *Appl. Catal. B Environ.* **70**, 323–329 (2007).
13. Galbraith, D., Gross, S. A. & Paustenbach, D. Benzene and human health: A historical review and appraisal of associations with various diseases. *Crit. Rev. Toxicol.* **40**, 1–46 (2010).
14. Faustini, A., Rapp, R. & Forastiere, F. Nitrogen dioxide and mortality: review and meta-analysis of long-term studies. *Eur. Respir. J.* **44**, 744–753 (2014).
15. Kircher, M. White biotechnology: Ready to partner and invest in. *Biotechnol. J.* **1**, 787–794 (2006).
16. Keasling, J. D. Manufacturing molecules through metabolic engineering. *Science* **330**, 1355–8 (2010).
17. Krivoruchko, A., Siewers, V. & Nielsen, J. Opportunities for yeast metabolic engineering: Lessons from synthetic biology. *Biotechnol. J.* **6**, 262–276 (2011).

18. Yan, Y. & Liao, J. C. Engineering metabolic systems for production of advanced fuels. *J. Ind. Microbiol. Biotechnol.* **36**, 471–9 (2009).
19. Lee, S. K., Chou, H., Ham, T. S., Lee, T. S. & Keasling, J. D. Metabolic engineering of microorganisms for biofuels production: from bugs to synthetic biology to fuels. *Curr. Opin. Biotechnol.* **19**, 556–563 (2008).
20. Suriyamongkol, P., Weselake, R., Narine, S., Moloney, M. & Shah, S. Biotechnological approaches for the production of polyhydroxyalkanoates in microorganisms and plants - a review. *Biotechnol. Adv.* **25**, 148–75 (2007).
21. Hempel, F. *et al.* Microalgae as bioreactors for bioplastic production. *Microb. Cell Fact.* **10**, 81 (2011).
22. Ohnishi, J. *et al.* A novel methodology employing *Corynebacterium glutamicum* genome information to generate a new L-lysine-producing mutant. *Appl. Microbiol. Biotechnol.* **58**, 217–223 (2002).
23. Becker, J. & Wittmann, C. Systems and synthetic metabolic engineering for amino acid production - the heartbeat of industrial strain development. *Curr. Opin. Biotechnol.* **23**, 718–726 (2012).
24. Jeandet, P., Vasserot, Y., Chastang, T. & Courot, E. Molecular Engineering of Microbes for the Biosynthesis of Natural Compounds of Pharmaceutical Significance. *Biomed Res. Int.* **2013**, 1–35 (2013).
25. Fossati, E. *et al.* Reconstitution of a 10-gene pathway for synthesis of the plant alkaloid dihydrosanguinarine in *Saccharomyces cerevisiae*. *Nat Commun* **5**, (2014).
26. Facchini, P. J. *et al.* Synthetic biosystems for the production of high-value plant metabolites. *Trends Biotechnol.* **30**, 127–131 (2012).
27. Demirbas, F., Balat, M. & Balat, H. Potential contribution of biomass to the sustainable energy development. *Energy Convers. Manag.* **50**, 1746–1760 (2009).
28. Renewable Energy Resources Map USDA.

29. Ragauskas, A. J. *et al.* The path forward for biofuels and biomaterials. *Science* (80-.). **311**, 484–9 (2006).
30. Cheng, Q., Thomas, S. M. & Rouvière, P. Biological conversion of cyclic alkanes and cyclic alcohols into dicarboxylic acids: Biochemical and molecular basis. *Appl. Microbiol. Biotechnol.* **58**, 704–711 (2002).
31. Steffensen, W. S. & Alexander, M. Role of competition for inorganic nutrients in the biodegradation of mixtures of substrates. *Appl. Environ. Microbiol.* **61**, 2859–2862 (1995).
32. Brzostowicz, P. C., Gibson, K. L., Thomas, S. M., Blasko, M. S. & Rouvière, P. E. Simultaneous identification of two cyclohexanone oxidation genes from an environmental *Brevibacterium* isolate using mRNA differential display. *J. Bacteriol.* **182**, 4241–4248 (2000).
33. Brzostowicz, P. C., Walters, D. M., Thomas, S. M., Nagarajan, V. & Rouvière, P. E. mRNA differential display in a microbial enrichment culture: Simultaneous identification of three cyclohexanone monooxygenases from three species. *Appl. Environ. Microbiol.* **69**, 334–342 (2003).
34. Cao, B., Geng, A. & Loh, K. C. Induction of ortho- and meta-cleavage pathways in *Pseudomonas* in biodegradation of high benzoate concentration: MS identification of catabolic enzymes. *Appl. Microbiol. Biotechnol.* **81**, 99–107 (2008).
35. Deneff, V. J. *et al.* Genetic and genomic insights into the role of benzoate-catabolic pathway redundancy in *Burkholderia xenovorans* LB400. *Appl. Environ. Microbiol.* **72**, 585–595 (2006).
36. Collier, L. S., Gaines, G. L. & Neidle, E. L. Regulation of benzoate degradation in *Acinetobacter* sp. strain ADP1 by BenM, a LysR-type transcriptional activator. *J. Bacteriol.* **180**, 2493–2501 (1998).
37. Strachan, P. D., Freer, a a & Fewson, C. a. Purification and characterization of catechol 1,2-dioxygenase from *Rhodococcus rhodochrous* NCIMB 13259 and cloning and sequencing of its *catA* gene. *Biochem. J.* **333** (Pt 3, 741–747 (1998).
38. Thomas, J. M. *et al.* Bimetallic nanocatalysts for the conversion of muconic acid to adipic

- acid. *Chem. Commun. (Camb)*. 1126–1127 (2003). doi:10.1039/b300203a
39. Schmidt, E. & Knackmuss, H. Production of cis,cis-muconate from benzoate and 2-fluoro-cis,cis-muconate from 3-fluorobenzoate by 3-chlorobenzoate degrading bacteria. *Appl. Microbiol. Biotechnol.* 351–355 (1984).
 40. Bang, S. & Choi, C. Y. DO-stat fed-batch production of cis,cis-muconic acid from benzoic-acid by *Pseudomonas putida* BM014. *J. Ferment. Bioeng.* **79**, 381–383 (1995).
 41. Braus, G. H. Aromatic amino acid biosynthesis in the yeast *Saccharomyces cerevisiae*: a model system for the regulation of a eukaryotic biosynthetic pathway. *Microbiol. Rev.* (1991).
 42. Richards, T. a. *et al.* Evolutionary origins of the eukaryotic shikimate pathway: Gene fusions, horizontal gene transfer, and endosymbiotic replacements. *Eukaryot. Cell* **5**, 1517–1531 (2006).
 43. Gosset, G. Production of aromatic compounds in bacteria. *Curr. Opin. Biotechnol.* **20**, 651–658 (2009).
 44. Morden, C. W., Delwiche, C. F., Kuhsel, M. & Palmer, J. D. Gene phylogenies and the endosymbiotic origin of plastids. *BioSystems* **28**, 75–90 (1992).
 45. Hawkins, a R. & Smith, M. Domain structure and interaction within the pentafunctional arom polypeptide. *Eur. J. Biochem.* **196**, 717–724 (1991).
 46. Hansen, E. H. *et al.* De novo biosynthesis of vanillin in fission yeast (*Schizosaccharomyces pombe*) and baker's yeast (*Saccharomyces cerevisiae*). *Appl. Environ. Microbiol.* **75**, 2765–74 (2009).
 47. McKenna, R., Thompson, B., Pugh, S. & Nielsen, D. R. Rational and combinatorial approaches to engineering styrene production by *Saccharomyces cerevisiae*. *Microb. Cell Fact.* **13**, 123 (2014).
 48. Draths, K. M., Frost, J. W. & Indiana, W. L. Environmentally Compatible Synthesis of Adipic Acid from &Glucose. *J. Am. Chem. SOC* 399–400 (1994). doi:10.1021/ja00080a057

49. Luttik, M. a H. *et al.* Alleviation of feedback inhibition in *Saccharomyces cerevisiae* aromatic amino acid biosynthesis: quantification of metabolic impact. *Metab. Eng.* **10**, 141–53 (2008).
50. Sprenger, G. a. From scratch to value: Engineering *Escherichia coli* wild type cells to the production of L-phenylalanine and other fine chemicals derived from chorismate. *Appl. Microbiol. Biotechnol.* **75**, 739–749 (2007).
51. Weaver, L. M. & Herrmann, K. M. Cloning of an *aroF* allele encoding a tyrosine-insensitive 3-deoxy-D-arabino-heptulosonate 7-phosphate synthase. *J. Bacteriol.* **172**, 6581–6584 (1990).
52. Li, K., Mikola, M. R., Draths, K. M., Worden, R. M. & Frost, J. W. Fed-batch fermentor synthesis of 3-dehydroshikimic acid using recombinant *Escherichia coli*. *Biotechnol. Bioeng.* **64**, 61–73 (1999).
53. Garner, C. C. & Herrmann, K. M. Operator mutations of the *Escherichia coli* *aroF* gene. *J. Biol. Chem.* **260**, 3820–3825 (1985).
54. Sun, X., Lin, Y., Huang, Q., Yuan, Q. & Yan, Y. A novel muconic acid biosynthesis approach by shunting tryptophan biosynthesis via anthranilate. *Appl. Environ. Microbiol.* **79**, 4024–4030 (2013).
55. Lin, Y., Sun, X., Yuan, Q. & Yan, Y. Extending shikimate pathway for the production of muconic acid and its precursor salicylic acid in *Escherichia coli*. *Metab. Eng.* **23**, 62–69 (2014).
56. Gaille, C., Reimmann, C. & Haas, D. Isochorismate synthase (PchA), the first and rate-limiting enzyme in salicylate biosynthesis of *Pseudomonas aeruginosa*. *J. Biol. Chem.* **278**, 16893–16898 (2003).
57. Gaille, C., Kast, P. & Dieter, H. Salicylate biosynthesis in *Pseudomonas aeruginosa*. Purification and characterization of PchB, a novel bifunctional enzyme displaying isochorismate pyruvate-lyase and chorismate mutase activities. *J. Biol. Chem.* **277**, 21768–21775 (2002).
58. Lin, Y., Shen, X., Yuan, Q. & Yan, Y. Microbial biosynthesis of the anticoagulant precursor 4-hydroxycoumarin. *Nat Commun* **4**, (2013).

59. Wang, J. & Zheng, P. Muconic acid production from glucose using enterobactin precursors in *Escherichia coli*. *J. Ind. Microbiol. Biotechnol.* (2015). doi:10.1007/s10295-014-1581-6
60. Sun, X., Lin, Y., Yuan, Q. & Yan, Y. Biological Production of Muconic Acid via a Prokaryotic 2,3-Dihydroxybenzoic Acid Decarboxylase. *ChemSusChem* **7**, 2478–2481 (2014).
61. SHERMAN, F. in *The Encyclopedia of Molecular Biology and Molecular Medicine* (ed. Meyers, R. A.) 302–325 (VCH, 1997).
62. Wickner, R. B. Double-Stranded RNA Viruses of *Saccharomyces cerevisiae*. *Microbiol. Rev.* **60**, 250–265 (1996).
63. Liu, C.-G., Wang, N., Lin, Y.-H. & Bai, F.-W. Very high gravity ethanol fermentation by flocculating yeast under redox potential-controlled conditions. *Biotechnol. Biofuels* **5**, 61 (2012).
64. Pinel, D. *et al.* *Saccharomyces cerevisiae* genome shuffling through recursive population mating leads to improved tolerance to spent sulfite liquor. *Appl. Environ. Microbiol.* **77**, 4736–4743 (2011).
65. Zhao, X. Q. & Bai, F. W. Mechanisms of yeast stress tolerance and its manipulation for efficient fuel ethanol production. *J. Biotechnol.* **144**, 23–30 (2009).
66. Westfall, P. J. *et al.* From the Cover: PNAS Plus: Production of amorphadiene in yeast, and its conversion to dihydroartemisinic acid, precursor to the antimalarial agent artemisinin. *Proceedings of the National Academy of Sciences* (2012). doi:10.1073/pnas.1110740109
67. Weber, C. *et al.* Biosynthesis of cis,cis-muconic acid and its aromatic precursors, catechol and protocatechuic acid, from renewable feedstocks by *saccharomyces cerevisiae*. *Appl. Environ. Microbiol.* **78**, 8421–8430 (2012).
68. Duncan, K., Edwardst, R. M. & John, R. The Pentafuntional arom enzyme of *Saccharomyces cerevisiae* is a mosaic of monofunctional domains. *J. Biochem.* **246**, 375–386 (1987).

69. Curran, K. a., Leavitt, J. M., Karim, A. S. & Alper, H. S. Metabolic engineering of muconic acid production in *Saccharomyces cerevisiae*. *Metab. Eng.* **15**, 55–66 (2013).
70. Bro, C., Regenberg, B., Förster, J. & Nielsen, J. In silico aided metabolic engineering of *Saccharomyces cerevisiae* for improved bioethanol production. *Metab. Eng.* **8**, 102–111 (2006).
71. Asadollahi, M. a. *et al.* Enhancing sesquiterpene production in *Saccharomyces cerevisiae* through in silico driven metabolic engineering. *Metab. Eng.* **11**, 328–334 (2009).
72. Zheng, Y. & Sriram, G. Mathematical modeling: Bridging the gap between concept and realization in synthetic biology. *J. Biomed. Biotechnol.* **2010**, (2010).
73. Misra, A. *et al.* Metabolic analyses elucidate non-trivial gene targets for amplifying dihydroartemisinic acid production in yeast. *Front. Microbiol.* **4**, 1–15 (2013).
74. Melzer, G., Esfandabadi, M. E., Franco-Lara, E. & Wittmann, C. Flux Design: In silico design of cell factories based on correlation of pathway fluxes to desired properties. *BMC Syst. Biol.* **3**, 120 (2009).
75. Mo, M. L., Palsson, B. O. & Herrgård, M. J. Connecting extracellular metabolomic measurements to intracellular flux states in yeast. *BMC Syst. Biol.* **3**, 37 (2009).
76. Sprenger, G. a., Schorken, U., Sprenger, G. & Sahm, H. Transketolase A of *Escherichia coli* K12 - Purification and properties of the enzyme from recombinant strains. *Eur. J. Biochem.* **230**, 525–532 (1995).
77. Horwitz, A. A. *et al.* Efficient Multiplexed Integration of Synergistic Alleles and Metabolic Pathways in Yeasts via CRISPR-Cas. *Cell Syst.* **1**, 88–96 (2015).
78. Ellis, R. J. Macromolecular crowding: Obvious but underappreciated. *Trends Biochem. Sci.* **26**, 597–604 (2001).
79. Kao, H. P. & Abney, J. R. Determinants of the Translational Mobility of a Small Solute in Cell Cytoplasm. *J. Cell Biol.* **120**, 175–184 (1993).

80. Winkel, B. S. J. Metabolic channeling in plants. *Annu. Rev. Plant Biol.* **55**, 85–107 (2004).
81. Miles, E. W., Rhee, S. & Davies, D. R. The Molecular Basis of Substrate Channeling. *J. Biol. Chem.* **274**, 12193–12196 (1999).
82. Conrado, R. J., Varner, J. D. & DeLisa, M. P. Engineering the spatial organization of metabolic enzymes: mimicking nature's synergy. *Curr. Opin. Biotechnol.* **19**, 492–9 (2008).
83. Dunn, M. F., Niks, D., Ngo, H., Barends, T. R. M. & Schlichting, I. Tryptophan synthase: the workings of a channeling nanomachine. *Trends Biochem. Sci.* **33**, 254–264 (2008).
84. Barends, T. R., Dunn, M. F. & Schlichting, I. Tryptophan synthase, an allosteric molecular factory. *Curr. Opin. Chem. Biol.* **12**, 593–600 (2008).
85. Lamb, H. K. *et al.* Differential flux through the quinate and shikimate pathways. Implications for the channelling hypothesis. *Biochem. J.* **284** (Pt 1, 181–187 (1992).
86. Hawkins, a R., Moore, J. D. & Lamb, H. K. The molecular biology of the pentafunctional AROM protein. *Biochem. Soc. Trans.* **21**, 181–186 (1993).
87. Singh, S. A. & Christendat, D. Structure of Arabidopsis dehydroquinate dehydratase-shikimate dehydrogenase and implications for metabolic channeling in the shikimate pathway. *Biochemistry* **45**, 7787–7796 (2006).
88. Park, A. *et al.* Biophysical and kinetic analysis of wild-type and site-directed mutants of the isolated and native dehydroquinate synthase domain of the AROM protein. *Protein Sci.* **13**, 2108–2119 (2004).
89. Hawkins, a R., Moore, J. D. & Adeokun, a M. Characterization of the 3-dehydroquinase domain of the pentafunctional AROM protein, and the quinate dehydrogenase from *Aspergillus nidulans*, and the overproduction of the type II 3-dehydroquinase from *neurospora crassa*. *Biochem. J.* **296** (Pt 2, 451–457 (1993).
90. Moore, J. D. & Hawkins, A. R. Overproduction of, and interaction within, bifunctional

- domains from the amino- and carboxy-termini of the pentafunctional AROM protein of *Aspergillus nidulans*. *Mol. Gen. Genet.* **303**, 297–303 (1993).
91. Horwitz, A. A. *et al.* Efficient Multiplexed Integration of Synergistic Alleles and Metabolic Pathways in Yeasts via CRISPR-Cas. *Cell Syst.* 1–9 (2015). doi:10.1016/j.cels.2015.02.001
 92. Winzeler, E. A. *et al.* Functional Characterization of the *S. cerevisiae* Genome by Gene Deletion and Parallel Analysis. *Sci.* **285**, 901–906 (1999).
 93. Portnoy, V. A., Bezdán, D. & Zengler, K. Adaptive laboratory evolution--harnessing the power of biology for metabolic engineering. *Curr. Opin. Biotechnol.* **22**, 590–4 (2011).
 94. Çakar, Z. P., Seker, U. O. S., Tamerler, C., Sonderegger, M. & Sauer, U. Evolutionary engineering of multiple-stress resistant *Saccharomyces cerevisiae*. *FEMS Yeast Res.* **5**, 569–578 (2005).
 95. Reyes, L. H., Gomez, J. M. & Kao, K. C. Improving carotenoids production in yeast via adaptive laboratory evolution. *Metab. Eng.* **21**, 26–33 (2014).
 96. Ye, S. *et al.* The crystal structure of shikimate dehydrogenase (AroE) reveals a unique NADPH binding mode. *J. Bacteriol.* **185**, 4144–4151 (2003).
 97. Michel, G. *et al.* Structures of shikimate dehydrogenase AroE and its paralog YdiB: A common structural framework for different activities. *J. Biol. Chem.* **278**, 19463–19472 (2003).
 98. Singh, S. *et al.* Crystal structure of a novel shikimate dehydrogenase from *Haemophilus influenzae*. *J. Biol. Chem.* **280**, 17101–17108 (2005).
 99. Han, C. *et al.* X-ray crystallographic and enzymatic analyses of shikimate dehydrogenase from *Staphylococcus epidermidis*: Implications for substrate binding and conformational change. *FEBS J.* **276**, 1125–1139 (2009).
 100. Reményi, A., Schöler, H. R. & Wilmanns, M. Combinatorial control of gene expression. *Nat. Struct. Mol. Biol.* **11**, 812–815 (2004).

101. Grilly, C., Stricker, J., Pang, W. L., Bennett, M. R. & Hasty, J. A synthetic gene network for tuning protein degradation in *Saccharomyces cerevisiae*. *Mol. Syst. Biol.* **3**, 127 (2007).
102. Zhou, P. & Howley, P. M. Ubiquitination and degradation of the substrate recognition subunits of SCF ubiquitin-protein ligases. *Mol. Cell* **2**, 571–80 (1998).
103. Yaglom, J. *et al.* p34Cdc28-mediated control of Cln3 cyclin degradation. *Mol. Cell. Biol.* **15**, 731–41 (1995).
104. Enserink, J. M. & Kolodner, R. D. An overview of Cdk1-controlled targets and processes. *Cell Div.* **5**, 11 (2010).
105. Salama, S. R., Hendricks, K. B. & Thorner, J. G1 cyclin degradation: the PEST motif of yeast Cln2 is necessary, but not sufficient, for rapid protein turnover. *Mol. Cell. Biol.* **14**, 7953–7966 (1994).
106. Mateus, C. & Avery, S. V. Destabilized green fluorescent protein for monitoring dynamic changes in yeast gene expression with flow cytometry. *Yeast* (2000). doi:10.1002/1097-0061(200010)16:14<1313::AID-YEA626>3.0.CO;2-O
107. Larionov, V. *et al.* Transformation-associated recombination between diverged and homologous DNA repeats is induced by strand breaks. *Yeast* **10**, 93–104 (1994).
108. Melcher, K. A modular set of prokaryotic and eukaryotic expression vectors. *Anal. Biochem.* **277**, 109–20 (2000).
109. Jansen, G., Wu, C., Schade, B., Thomas, D. Y. & Whiteway, M. Drag&Drop cloning in yeast. *Gene* **344**, 43–51 (2005).
110. Entian, K.-D. & Kötter, P. *Yeast Genetic Strain and Plasmid Collections. Methods in Microbiology* **36**, (Elsevier, 2007).
111. Gietz, R. D. & Schiestl, R. H. High-efficiency yeast transformation using the LiAc/SS carrier DNA/PEG method. *Nat. Protoc.* **2**, 31–34 (2007).
112. Güldener, U., Heck, S., Fiedler, T., Beinhauer, J. & Hegemann, J. H. A new efficient gene

- disruption cassette for repeated use in budding yeast. *Nucleic Acids Res.* **24**, 2519–2524 (1996).
113. Sherman, F. Getting Started with Yeast. *Methods Enzymol.* **350**, 3–41 (2002).
 114. Gibson, D. G. *et al.* Enzymatic assembly of DNA molecules up to several hundred kilobases. **6**, 12–16 (2009).
 115. Dicarlo, J. E. *et al.* Genome engineering in *Saccharomyces cerevisiae* using CRISPR-Cas systems. *Nucleic Acids Res.* **41**, 4336–4343 (2013).
 116. Roon, R. J., Larimore, F. & Levy, J. S. Inhibition of amino acid transport by ammonium ion in *Saccharomyces cerevisiae*. *J. Bacteriol.* **124**, 325–331 (1975).
 117. Daran-Lapujade, P. *et al.* Comparative genotyping of the *Saccharomyces cerevisiae* laboratory strains S288C and CEN.PK113-7D using oligonucleotide microarrays. *FEMS Yeast Res.* **4**, 259–269 (2003).
 118. Xu, Y. F. *et al.* Regulation of Yeast Pyruvate Kinase by Ultrasensitive Allosteric Independent of Phosphorylation. *Mol. Cell* **48**, 52–62 (2012).